Information Fusion 97 (2023) 101806

Contents lists available at ScienceDirect

Information Fusion

journal homepage: www.elsevier.com/locate/inffus

Full length article

External multi-modal imaging sensor calibration for sensor fusion: A review

Zhouyan Qiu [a,b,*], Joaquín Martínez-Sánchez [a], Pedro Arias-Sánchez [a], Rabia Rashdi [a,b]

[a] CINTECX, Universidade de Vigo, Applied Geotechnology Group, Vigo, 36310, Spain
[b] ICT & Innovation Department, Ingeniería Insitu, Vigo, 36310, Spain

ARTICLE INFO

Keywords:
Multi-modal
Sensor calibration
LiDAR
Camera
Sensor fusion
Mobile mapping

ABSTRACT

Multi-modal data fusion has gained popularity due to its diverse applications, leading to an increased demand for external sensor calibration. Despite several proven calibration solutions, they fail to fully satisfy all the evaluation criteria, including accuracy, automation, and robustness. Thus, this review aims to contribute to this growing field by examining recent research on multi-modal imaging sensor calibration and proposing future research directions. The literature review comprehensively explains the various characteristics and conditions of different multi-modal external calibration methods, including traditional motion-based calibration and feature-based calibration. Target-based calibration and targetless calibration are two types of feature-based calibration, which are discussed in detail. Furthermore, the paper highlights systematic calibration as an emerging research direction. Finally, this review concludes crucial factors for evaluating calibration methods and provides a comprehensive discussion on their applications, with the aim of providing valuable insights to guide future research directions. Future research should focus primarily on the capability of online targetless calibration and systematic multi-modal sensor calibration.

1. Introduction

Multi-modal imaging sensor fusion refers to bringing together complementary and sometimes competing sensory data into a reliable environment estimate to achieve a result that is greater than the sum of its parts (Hackett and Shah [1]). In recent years, with sensor technology development, multi-modal learning plays an increasingly important role in remote sensing (Luo et al. [2]), robotics (Nagla et al. [3]), indoor and outdoor Simultaneous Localization and Mapping (SLAM) (Van Dinh and Kim [4]), intelligent transport infrastructure (Soilán et al. [5]), Building Information Modelling (BIM) (Rashdi et al. [6]), and autonomous driving (Trubia et al. [7]). There are three different types of sensor fusion, which refers to three different data processing levels of abstraction: data-level fusion, feature-level fusion, and decision-level fusion (Hall and Llinas [8]). We consider data-level fusion and feature-level fusion as early fusion, and decision-level fusion as late fusion. Early fusion denotes the integration of the data from the input (Kumar et al. [9]). In contrast, late fusion, also known as decision-level fusion, differs from early fusion by performing classification or recognition independently by each sensor. The integration of data series is done at the semantic level. Therefore, synchronization and calibration are not required in late-level fusion, but they are necessary requirements of early level fusion. It is necessary to regularize input sources from different sensors when performing data-level and feature-level fusion. The goal of regularization is to achieve the same goal simultaneously with different types of sensors appearing in the same coordinate system. Therefore, the calibration of multi-modal sensors is an essential component of multi-view learning and applications.

The purpose of multi-modal sensors calibration is to determine how data from different sources can be transformed into a common reference system that is necessary for early-level sensor fusion. There are two types of multi-sensor calibration (Kummerle and Kuhner [10]): intrinsic calibration and extrinsic calibration. Intrinsic calibration determines the internal mapping relationship of the sensor, for example, the focal length, eccentricity, and pixel aspect ratio of the camera (Pollefeys et al. [11]), and the lever-arm vector and bore-sight angles of the LiDAR (Skaloud and Lichti [12]). Extrinsic calibration defines the sensor poses relative to the reference frame.

A majority of multi-modal sensors are supplied with intrinsic calibration parameters by the manufacturer or are calculated independently. Therefore, the primary purpose of multi-sensor calibration is extrinsic calibration. In extrinsic calibration, usually, the relative pose is represented by the homogeneous transformation matrix, which transforms the same point from one reference frame to another. As can be seen in Eq. (1.1), it is possible to combine translation, rotation, scaling, reflection, and shear in a single 4×4 transformation matrix in 3D space. The 3×3 matrix R is the rotation matrix, describing the sensors' rotation or orientation (and also scales and shears in some cases). The

* Corresponding author at: CINTECX, Universidade de Vigo, Applied Geotechnology Group, Vigo, 36310, Spain.
E-mail address: zhouyan.qiu@uvigo.es (Z. Qiu).

https://doi.org/10.1016/j.inffus.2023.101806
Received 16 January 2023; Received in revised form 3 April 2023; Accepted 6 April 2023
Available online 12 April 2023

3×1 matrix T is the translation matrix, representing the displacement relationship between sensors.

Recent research simultaneously calibrates the entire multi-modal sensor system, allowing it to solve both intrinsic and extrinsic calibration parameters at the same time. This part will be discussed in Section 5.

If we only take the rotation into consideration, then the Matrix R is orthonormal. According to Euler's rotation theorem, any rotation in 3D space is represented by rotating a unit vector $\vec{u}$ (the Euler axis) through a certain angle θ. Quaternions (Brauner [13]) describe the axis-angle representation in four variables. A quaternion rotation is algebraically manipulated into a matrix rotation by Eq. (1.1) (O'Rourke [14]).

Here, $s = \|q\|^{-2}$ and if q is a unit quaternion, $s = 1$. Therefore, the task of extrinsic calibration is simplified to find seven unknown parameters, including a 1×4 rotation quaternion vector $\mathbf{q} = \left(q_i, q_j, q_k, q_r\right)$ and a 1×3 translation vector $\mathbf{T}$. A transformation converts a 3D point coordinates $\mathbf{P}_1 = \left[X_1, Y_1, Z_1\right]^T$ in sensor 1 coordinate system to coordinates $\mathbf{P}_2 = \left[X_2, Y_2, Z_2\right]^T$ in sensor 2 coordinate system using Eq. (1.1).

$$\begin{bmatrix} \mathbf{P}_1 \\ 1 \end{bmatrix} = \begin{bmatrix} \mathbf{R}_{3\times3} & \mathbf{T}_{3\times1} \\ 0_{1\times3} & 1 \end{bmatrix} \begin{bmatrix} \mathbf{P}_2 \\ 1 \end{bmatrix}, \text{ or } : \mathbf{P}_1 = \mathbf{R}_{3\times3} \cdot \mathbf{P}_2 + \mathbf{T}_{3\times1} \quad (1.1)$$

It is difficult to obtain all the corresponding sensor values simultaneously in a multi-modal sensor system because of the different sample rates, field of views (FoVs). and resolution. As a prerequisite to multi-view learning, robustness and accuracy are additional requirements for sensor calibration. It is therefore not an easy task to calibrate multi-modal sensors at the production level.

There has been no decline in the popularity of multi-modal sensor calibration within the last 20 years, but rather it has become more significant with the needs of research directions such as unmanned driving and mobile mapping. We review the popular multi-sensor calibration problem where no systematic reviews published in recent years. In our review, we cited more than 250 papers, of which over 90 were published within the last three years and almost 130 within the last five years.

This paper aims to present a comprehensive overview of the existing external imaging sensor calibration approaches. The structure of the paper includes seven sections. The first section is the introduction, which provides an overview of the paper. Section 2 discusses the fundamentals of external multi-modal image sensor calibration, including an overview of multi-modal imaging sensors, prerequisites such as time synchronization and motion compensation, and the general process of external multi-modal sensor calibration. Sections 3 and 4 present motion-based calibration and feature-based calibration methods, respectively. Section 5 provides an overview of systematic multi-modal sensor calibration. In Section 6, the key factors for evaluating calibration methods in multi-modal sensor systems are discussed, along with their advantages, disadvantages and related applications. Additionally, potential research directions are highlighted. Finally, Section 7 concludes the paper.

2. Fundamentals of external multi-modal image sensor calibration

The section begins by providing an overview of multi-modal imaging sensors, including camera, LiDAR and Radar. It then moves on to discuss the prerequisites of external multi-modal imaging sensor calibration, including time synchronization and motion compensation, which are essential for achieving accurate calibration. The final part of the section explains the general process of external multi-modal sensor calibration, providing an overview of the various steps involved in the calibration process. Overall, this section provides an introductory overview of the fundamental concepts and techniques utilized in multi-modal imaging sensor calibration.

2.1. Overview of multi-model imaging sensors

Over the past decades, many multi-modal sensor datasets have been released for multiple purposes including detection, tracking, prediction and segmentation (Caesar et al. [15]). In 2006, the Rawseeds project published the first multi-sensor indoor and outdoor datasets (Bonarini et al. [16]). Table 2.1 lists the open-source multi-modal sensor datasets and the sensors they use (until 2022.08). As can be seen from Table 2.1, GPS and IMU (inertial measurement unit) are essential for time synchronization and sensor calibration part. Many datasets, such as MVSEC (Zhu et al. [17]) and CADC (Pitropov et al. [18]), are equipped with multiple GNSS and IMU sensors to resolve synchronization problems. Sometimes the dataset providers have completed the multi-sensor calibration for users. For example, the calibration files of the popular KITTI (Geiger et al. [19]) dataset is available online. However, it is not accurate enough for specific objectives, e.g., high-precision map positioning. Thus, there are many sensor calibration processes based on the KITTI dataset (Feng et al. [20], Jiang et al. [21]). In addition to LiDARs and cameras, researchers have also begun to use other sensors, such as radars (Houston et al. [22], Caesar et al. [15], Barnes et al. [23]), thermal (Choi et al. [24]) and fisheye cameras (Yogamani et al. [25]).

2.1.1. Camera

Cameras are the basis of the visual image processing system and the foundation of the multi-sensor platform. In addition to the frequently chosen grey-scale cameras and color cameras, video cameras are often utilized for 3D target tracking and positioning. Furthermore, depending on the purpose, some specific cameras are also valuable to multi-sensor fusion such as Stereo cameras, panoramic cameras, fisheye cameras, ToF cameras, thermographic camera, multi-spectral cameras. The comparisons of various popular cameras are presented in Table 2.2.

Besides the above frame cameras, line scan cameras have one or more rows of imaging units on their sensors, which are considered as a particular case of frame cameras. A line scan camera has a higher scanning frequency and resolution. It is vital to maintain the relative movement between the camera and the object when employing line frame cameras to collect 2D images. Because it only images line objects, calibrating a line scan camera is more difficult than calibrating a frame camera. Static and dynamic imaging methods are now used to calibrate line scan cameras.

- Static imaging methods: keep the camera and calibration object motionless, and each row of data on the image surface is consistent (Horaud et al. [69], Li et al. [70], Sun et al. [71]).
- Dynamic scanning imaging: moves the line camera at a constant speed to create a 2D image, which is useful for extracting the pixel coordinates of the subsequent feature points (Draréni et al. [72], Hui et al. [73], Donné et al. [74]).

Due to the particularity of line scan cameras, the joint calibration of line scan cameras and other sensors are out of scope in this paper.

2.1.2. LiDAR

LiDAR, short for Light Detection and Ranging, is a device that measures the distance from the device to targets by the time-of-flight (TOF) or phase (Stone et al. [75]). According to the scanning methods, LiDARs are divided into three categories: Mechanical Scanning, Micro electromechanical system (MEMS) and solid-state. Mechanical Scanning LiDAR mechanically rotates a laser/receiver assembly or utilizing a spinning mirror to direct a light beam. MEMS LiDAR is a hybrid LiDAR that combines a MEMS with a Laser galvanometer to perform laser scanning through galvanometer rotation. Solid-state LiDAR has no mechanical scanning structures, and the laser scanning process is entirely electronic. Optical Phased Array (OPA) LiDAR and Area Array Flash LiDAR are two main types of solid-state LiDAR. Table 2.3 compares the advantages and the disadvantages of these LiDARs. According

Table 2.1
Public multi-sensor datasets for calibration (until 2022).

Dataset	Year	Environment	RGB	Other camera	LIDAR	IMU	GNSS	Radar
Bovisa [16]	2009	Outdoor	Multi		Yes	Yes	Yes	No
DARPA [26]	2010	Outdoor	Multi		Yes	Yes	Yes	No
KITTI [19]	2011	Outdoor	2		Yes	Yes	Yes	No
TUMindoor [27]	2012	Indoor	8		No	No	No	No
Málaga [28]	2013	Outdoor	1		Yes	Yes	Yes	No
NCLT [29]	2015	Outdoor	1		Yes	Yes	Yes	No
EUROC [30]	2016	Outdoor			No	No	No	No
LaFiDa [31]	2017	Indoor/Outdoor	3		No	No	No	No
TUM VI [32]	2018	Indoor/Outdoor	Multi	event	No	Yes	No	No
HDD [33]	2018	Outdoor	Multi		Yes	Yes	Yes	No
KAIST Multi-spectral [24]	2018	Outdoor	Multi	IR	Yes	Yes	Yes	No
MVSEC [17]	2018	Outdoor	Multi		Yes	Yes	Yes	No
Brno Urban [34]	2019	Outdoor	Multi		Yes	Yes	Yes	No
UZH-FPV [35]	2019	Indoor/Outdoor	1	event	No	Yes	No	No
REAL3EXT [36]	2019	Indoor	Multi	IR, depth	No	No	No	No
ApolloScape [37]	2019	Outdoor	6		Yes	Yes	Yes	No
Argoverse [38]	2019	Outdoor	Multi		Yes	Yes	Yes	No
Waymo [39]	2019	Outdoor	Multi		Yes	Yes	Yes	No
WoodScape [25]	2019	Outdoor	Multi		Yes	Yes	Yes	No
UrbanLoco [40]	2020	Outdoor	Multi		Yes	Yes	Yes	No
Pit30M [41]	2020	Outdoor	1		Yes	Yes	Yes	No
OpenLORIS [42]	2020	Indoor	2	depth	No	Yes	No	No
A2D2 [43]	2020	Outdoor	6		Yes	Yes	Yes	No
A*3D [44]	2020	Outdoor	Multi		Yes	Yes	Yes	No
CADC [18]	2020	Outdoor	Multi		Yes	Yes	Yes	No
Cityscapes [45]	2020	Outdoor	2		Yes	Yes	Yes	No
Ford Multi-AV [45]	2020	Outdoor	Multi		Yes	Yes	Yes	No
Lyft Perception; Lyft Prediction [46][22]	2020	Outdoor	Multi		Yes	Yes	Yes	Yes
nuScenes [15]	2020	Outdoor	6		Yes	Yes	Yes	Yes
Pandaset [47]	2020	Outdoor	Multi		Yes	Yes	Yes	No
RobotCar [23]	2020	Outdoor	Multi		Yes	Yes	Yes	Yes
Apolloscape Inpainting [48]	2020	Outdoor	Multi		Yes	No	No	No
USVinland [49]	2021	Outdoor	Multi		Yes	Yes	Yes	Yes
JU-VNT [50]	2021	Indoor	1	IR, multi-spectral	No	No	No	No
CyborgLOC (Team) [51]	2021	Indoor	No	IR	No	Yes	Yes	No
NAVER LABS Localization Datasets [52]	2021	Indoor	10		Yes	No	No	No
CRUW [53]	2021	Outdoor	2		No	No	No	Yes
RadarScenes [54]	2021	Outdoor	1		No	Yes	Yes	Yes
Dsec [55]	2021	Outdoor	Multi	event	Yes	No	Yes	No
TUK Campus [56]	2021	Outdoor	Multi		Yes	Yes	Yes	No
M2DGR [57]	2021	Indoor/Outdoor	7	IR, event	Yes	Yes	Yes	No
WADS(Winter) [58]	2021	Outdoor	Multi	IR	Yes	No	No	No
ONCE [59]	2021	Outdoor	7		Yes	No	No	No
TUM-VIE [60]	2021	Indoor/Outdoor	2	IR, event	No	No	Yes	No
TIMo [61]	2022	Indoor	No	IR, depth	No	No	No	No
SELMA [62]	2022	Outdoor	7	depth, semantic	Yes	Yes	Yes	No
Rope3D [63]	2022	Outdoor	1	roadside cameras	Yes	Yes	Yes	No
Argoverse 2 [64]	2023	Outdoor	9		Yes	No	No	No

Table 2.2
The characteristics and applications of various popular cameras.

Cameras	Stereo cameras	Fisheye cameras	Thermographic cameras
Definition	A type of camera with two or more lenses with a separate image sensor or film frame for each lens	have an ultra wide-angle lens that produces strong visual distortion intended to create a wide panoramic or hemispherical image [65,66]	Create an image using infrared radiation
Advantages	Can simulate human binocular vision, Able to capture 3D images	Shorter focal length, wider perspective, Accommodate more scenery information	Sensitive to particular wavelengths
Disadvantages	Complex configuration and calibration, The depth range and accuracy are limited by the binocular baseline and resolution, very consuming computing resources	Not applicable to the perspective projection model, Need special distortion correction	Short measuring distance, poor contrast, high cost
Open datasets	Málaga [28], MVSEC [17], Bicocca [16], REAL3EXT [67]	WoodScape [68]	KAIST Multi-spectral [24](thermal), JU-VNT [50](near-infrared, thermal)

Table 2.3
The advantages and disadvantages of different LiDARs.

LiDAR	Advantages	Disadvantages
Mechanical Scanning LiDAR	360-degree field of view, relatively high accuracy	The more the beams, the larger the size; expensive
MEMS LiDAR	Relatively mature technology, relatively lower cost and higher accuracy, sensors can dynamically adjust the scanning method, for the objects that need to be identified	Complicated optical path, the vibration of the polarizer, the area of the polarizer limits laser scanning, laser reflections result in a low echo signal-to-noise ratio
OPA LiDAR	Simple structure and small size, fast scanning speed and high accuracy, good controllability	Small field of view, grating diffraction affects the result, poor signal to noise ratio
Flash LiDAR	No motion distortion, fast scanning speed	Small field of view, small detection range

to this table, Mechanical Scanning LiDAR has a large field of view and high accuracy, but is large and expensive. MEMS LiDAR on the other hand, has a relatively low cost and higher accuracy, however, it is prone to noise. Although OPA LiDAR is small and has high accuracy, its field of view is small and its noise level is high. The Flash LiDAR is capable of rapid scanning, but it has a small field of view and detection range. Therefore, a LiDAR must be selected according to the specific requirements.

2.1.3. Radar

Radar is a detection system that uses radio waves to determine the range, angle, or velocity of objects (Smith [76]). Usually, millimeter-wave radars are set in the multi-sensor platform. Millimeter-wave refers to electromagnetic waves with a wavelength between 1 mm and 10 mm, which means the frequency is between 300 GHz and 30 GHz. The millimeter-wave has a strong ability to penetrate fog, smoke, and dust, long transmission distance, and has stable performance. However, radar fails to recognize obstacles, so there is the potential for false detection. For the reasons stated, many multi-sensor systems use radars as additional sensors to improve the accuracy and accuracy of measurements, such as nuScenes (Caesar et al. [15]) and RobotCar (Barnes et al. [23]).

2.2. Prerequisites of external multi-modal imaging sensor calibration

2.2.1. Time synchronization

Sensor fusion requires time synchronization of several data streams with potentially different frequencies and latencies, which has a direct effect on the accuracy and performance of the system (Hu et al. [77]). It is possible to synchronize sensor data using either hardware or software. Hardware synchronization uses a unified clock to synchronize the timestamps of different sensors to synchronize sensor acquisition and measurement. Software synchronization attaches a timestamp to each sensor measurement to correct synchronization errors caused by inconsistent data acquisition frequencies of different sensors. In the past few years, it has become increasingly popular to integrate time synchronization into systematized temporal and spatial calibration, which is described in detail in Section 5.

- **Hardware synchronization.** The master time is used to synchronize the timestamps of different sensors since each sensor has its own timestamp. Furthermore, there is still a delay in data transfer between sensors due to the varied sampling frequency of each sensor. Therefore the nearest neighbor frame is identified by searching at neighboring timestamps. In most cases, GPS time is used as the master time for other sensors.
- **Software synchronization.** Two simple methods of time synchronization are the time index and time interpolation. **Time index** uses frequency information from different sources within a multi-modal system, based on a relation between the sampling rate of the sensor with the lowest sampling frequency. This method has a significant amount of inaccuracy. **Time interpolation** is a least-squares approach which is one of the most widely used method for synchronizing time. The observed data from one sensor are fitted to create a time curve, and then the value corresponding to the time of the other sensor is calculated (Blair et al. [78]). Other mature solutions exist for situations in which the frame rate does not have a multiple relationship between the sensors, or when the frame rate is unstable. For example, an extrapolation of high-precision observation data into low-precision time stamps is possible, such as the Taylor expansion algorithm (Huang et al. [79]), interpolation and extrapolation (Brownlee [80]). Based on the individual application and conditions, there are other methods of time synchronization. Olson [81] presented a passive synchronization algorithm for estimating time offsets when both device and sensor clocks drift, which is practical and feasible, however, only when the sensors observe overlapping events. Kelly et al. [82] identified the time delay calculation as a registration issue and attempted to find correspondences among the measurements of both sensors. Furthermore, Du et al. [83] presented a procedure for time synchronization based on point correspondence for the parametrization of curves. According to Liu et al. [84], the high update rate IMU served as a unified calibration reference, whilst other moderate and low-frequency target sensors were estimated in connection with the reference unit.

2.2.2. Motion compensation

In a multi-modal system, all sensors are fixed on a rigid body in motion, for example, a car or a train. Therefore, when the sensors collect the data, the vehicle is at different positions before and after the data acquisition, resulting in the misalignment of different local sensor coordinate systems. There are two sources of motion compensation:

1. **Ego Motion**: Gibson [85] described ego motion based on visual signals. Ego motion is the change in the gathered data caused by the sensor's own motion in a multi-modal system. Raudies and Neumann [86] evaluated different estimating ego-motion methods.
2. **Motion from others**: The change in the sensor's relative displacement caused by the target moving during the acquisition procedure.

It is necessary to apply motion compensation methods before the sensor fusion, especially for the sensors with low sampling rates, such as radars, cameras and some LiDARs. GNSS and IMU provide the vehicle's position shifts at different times of the movement for motion compensation. Based on the assumption of a constant speed of the sensor, the sensor position is calculated by point cloud registration. Commonly used methods include Iterative Closest Point(ICP) and related variants, e.g. Velocity updating Iterative Closest Point Algorithm(VICP) (Hong et al. [87]), or Approximate Nearest Neighbor Algorithms(ANN) (Liu et al. [88]). The ICP algorithm's drawback is that it accumulates error over time and is prone to being incorrect in fast motion; also, it fails if the point clouds are very sparse (Balazadegan Sarvrood et al. [89]). The odometer and IMU information are used to solve the sensor position problem. They are updated at a very high frequency, allowing it to precisely reflect the motion condition.

Also, the fusion approach employs data gathered by the camera or LiDAR to match to correct the location. Yang et al. [90] evaluated

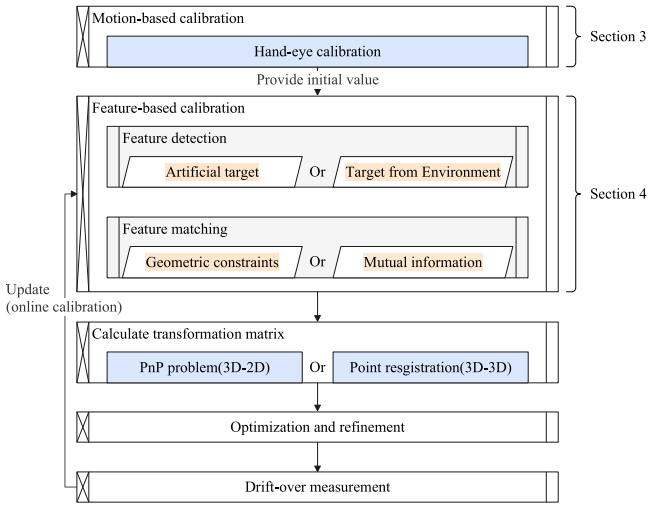

Fig. 2.1. A general process of external calibration in a multi-sensor platform.

the visual odometry algorithms using sophisticated achievements as an example to investigate the design ideas of various visual odometry methods. Many odometry and SLAM algorithms, such as ORB-SLAM (Mur-Artal et al. [91]) for monocular cameras, LOAM (Zhang and Singh [92]) for LiDARs, and RGBD-SLAM (Kerl et al. [93]) for RGBD sensors, have been developed in recent years to capture 3-D ego-motion with a specific exteroceptive sensor.

Furthermore, image blur reduction is sometimes referred to motion compensation in the field of computer vision due to sensor motions during exposure. This problem has a large number of well-developed solutions (Peng et al. [94], Har-Noy et al. [95], Couzinié-Devy et al. [96], Deshpande and Patnaik [97]). Besides, rolling shutter cameras rather than global shutter cameras are also beneficial in motion deblurring, which are usually applied in SLAM (Anderson and Barfoot [98], Patron-Perez et al. [99]). Based on simulations and real data, Huai et al. [100] quantified the rolling shutter effect on camera extrinsic and temporal calibration, and analyzed the effect of constant IMU bias assumption on extrinsic calibration.

2.3. General process of external multi-modal sensor calibration

Thus far, the prerequisites for calibration are outlined. The global calibration process is summarized in Fig. 2.1. While this process is a commonly adopted approach, it is important to note that it is not mandatory for all calibration methods to adhere to this scheme. In fact, many researchers have focused exclusively on specific aspects of the process. Some have focused exclusively on motion-based calibration methods, while others have assumed that the initial values are given before feature-based calibration methods. Additionally, some researchers have exclusively addressed the drift-over measurement problems for online processing. Despite these differences, the overall approach can be described as a coarse to fine calibration. For instance, motion-based hand-eye calibration provides only approximate extrinsic parameters. This allows it to contribute initial values for feature-based calibrations, which may also be assigned manually. After that, numerous optimization approaches are applied to increase the calibration accuracy after replicated measurements. In the case of multi-modal sensor systems, obtaining an accurate initial value is paramount, after which online calibration must be continuously performed to correct the external parameters of the sensors in motion. In the following sections, various calibration methods will be described separately.

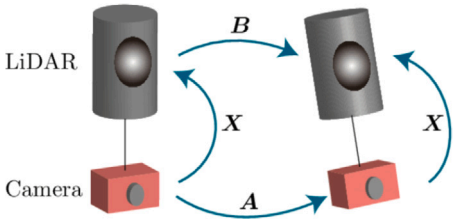

Fig. 3.1. Motion-based 2D–3D Calibration [103].

3. Motion-based calibration

Motion-based calibration techniques are based on the well-developed hand-eye calibration problem (Horaud and Dornaika [101]). In robotics and mathematics, the hand-eye calibration problem takes the form of $AX = ZB$, where A and B are two systems, and X and Z are unknown transformation matrices. In multi-sensor calibration, A and B are the motions of two sensors. Because here we require only the relative transformation matrices from A to B, we assume that here $X = Z$, taking the form of the problem $AX = XB$.

In hand-eye calibration, the movements of different sensors are used to calibrate external parameters (Fig. 3.1). As explained in the last paragraph, solving the expression for X in the equation $AX = XB$ provides the extrinsic parameter between the two sensors. Using this approach, researchers have been able to automatically initialize the external parameters in the case of non-overlapping FOVs (Taylor and Nieto [102], Ishikawa et al. [103]). In the motion-based calibration carried out by Ishikawa et al. [103], LiDAR motion is estimated by the ICP algorithm, while camera motion is calculated by feature matching. The initial calibration parameters can then be evaluated separately. Furthermore, the camera motion is recalculated by the initial external parameters and the point clouds. Finally, the external parameters can be achieved by hand-eye calibration.

As mentioned before, although motion-based calibration is a flexible targetless calibration method, the accuracy is not very high. Therefore, refinement after hand-eye calibration is necessary to improve the calibration accuracy. Generally, hand-eye calibration can provide initial values for feature-based target-less calibration or ICP optimization algorithms.

4. Feature-based calibration

One of the most important aspects of a multi-modal sensor calibration procedure is feature-based calibration. This process is accurate and straightforward to perform. Fig. 4.1 provides an overview of different features for various sensors. The most interesting aspect of this figure is that researchers often choose diverse targets according to the sensor's characteristics to facilitate external calibration. The commonly chosen targets are:

- **A checkerboard or a combination of checkerboards.** It is the most popular design. A preliminary inspection of the calibration object allows the corner position to be determined with a very high degree of accuracy. After the checkerboard is detected, subpixel refinement is possible by taking advantage of the precise gray values of pixels around a given corner position.
- **Sphere.** It is also a popular and prevalent calibration target design. A sphere is detected as a circle in the image. Since all pixels on the periphery of the circle are applied to reduce the influence of noise, it is possible to determine the circle with great accuracy. Another advantage of using the sphere is that the projection of the globe in any viewing angle is circular, so it is well adapted to non-overlapping views, which is very significant in practical applications.

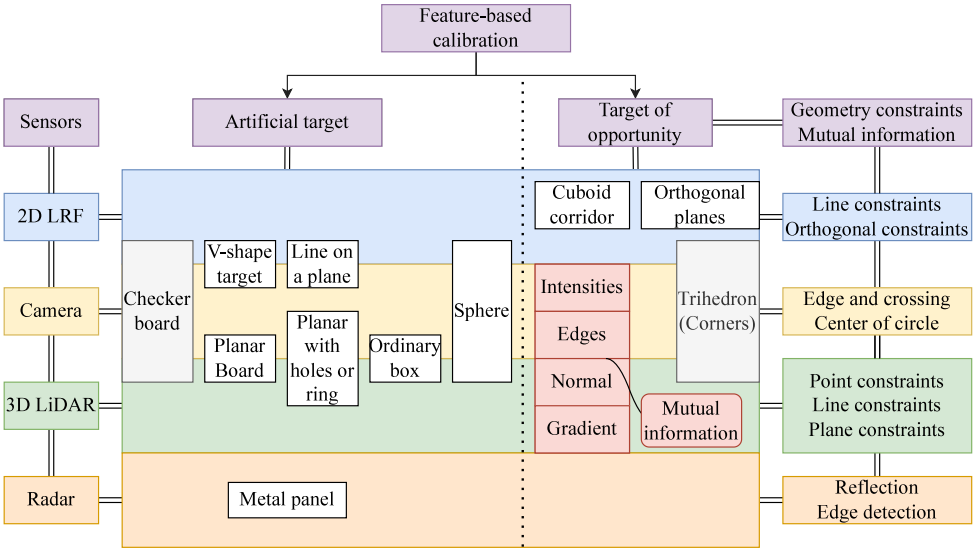

Fig. 4.1. Different feature-based calibration methods for different sensors according to their individual constraints.

- **Trihedron.** It is a commonly used non-artificial target, and it is frequently found in indoor or outdoor corners. The trihedrons provide not only line-based and plane-based restrictions but also orthogonal-based constraints. So, they give sufficient conditions for automatic calibration.

Closer inspection of Fig. 4.1 shows that in addition to target-based calibration methods, another calibration technique known as "target of opportunity" uses features from the environment to achieve calibration. There has been an increasing amount of literature on automatic calibration in recent years, taking advantage of geometry constraints or mutual information (MI). Without using human-made objects, effective features like points, lines, planes, and other features from the natural environment are extracted to achieve external parameter constraints and estimate the optimal parameters online in real-time, with stronger robustness and higher efficiency (Moghadam et al. [104], Levinson and Thrun [105], Rodríguez-Garavito et al. [106]). The generalizability of these approaches is subject to certain limitations. These methods are more suitable for indoor calibration because there are enough line features and surface features for self-correction. For outdoor cases, the sensors fail to obtain sufficient line and plane conditions. Han et al. [107] proposed an online calibration method based on traffic sign recognition, such as stop signs. This method is fast and efficient, but its application is limited. What is more, the complicated surrounding environment makes the automatic calibration result unstable.

The following is a brief introduction of feature-based calibration methods for different sensors, including multi-LiDAR, multi-camera, LiDAR and camera and others.

4.1. Feature-based multi-LiDAR calibration

Feature based multi-LiDAR calibration extract effective features from the scanned point cloud, such as the combined features of points, lines, arcs, and surfaces, the normal and curvature, and other customizable features. An example of customizable features is the field of view (FoV) overlaps created through sensor movements (Liu and Zhang [108]). For feature-based calibration, artificial targets (Gao and Spletzer [109], Chen et al. [110]) are usually set to obtain the correspondence, but in some papers, some specific features in the point clouds are directly detected for the calibration. Unlike 3D LiDARs, 2D Laser rangefinders (LRFs) do not provide height information as they are only capable of collecting distance information from one plane. Therefore, the calibration of multi-2D LRF systems is more difficult. Table 4.1 compares the strengths and weaknesses of some feature-based multi-LRFs calibration methods. As can be seen from Table 4.1, using artificial targets improves accuracy and calculation speed. Existing features, that are, geometric constraints, require a particular external environment and a large number of observations, but they are more flexible. Additionally, Chen et al. [111] proposed a feature extraction methodology that generalizes points' geometrical characteristics into two groups (disjoint and continuous) and three types (edge, corner, plane).

In addition, the dynamic features are used for the multi-LiDAR calibration problems. Schenk et al. [120] presented an automatic calibration methods of laser range finders by matching movement trajectories. However, it only solves the 3-DOFs extrinsic calibration problems, and the calibration error may be accumulated during the processing.

4.2. Feature-based multi-camera calibration

Feature-based multi-camera calibration has been very well developed since the beginning of the 21st century. Different feature-based multi-camera calibration methods are summarized in Table 4.2. From the table, it can be seen that most global calibration procedures in the early research rely on matching features in all sensor FoVs, requiring a common field of view.

Generally, the targets are categorized in terms of dimensions into 0D targets, 1D targets, 2D targets, and 3D targets (Table 4.2). A 0D target is a freely moving bright spot, which must be captured by at least three cameras (Svoboda et al. [121]). It is a self-calibration method finding the association among trajectories of a point across all views, mainly used for virtual environments. Therefore, it is not practical for outdoor applications.

The 1D calibration target comprises three or more collinear points with a known distance from each other (Zhang [122], Wu et al. [123], Wang and Wu [124]). The 1D target has two attractive features: first, its structure is simple and easy to set up; secondly, it has no occlusion, thus it is capable to be efficiently captured by multiple cameras. In a multi-camera system, all cameras observe the entire calibration object at the same time. But for 2D and 3D targets, it is impossible to realize due to their occlusion.

One of the greatest disadvantages of 1D targets is that they do not provide sufficient calibration constraints. One-dimensional targets are only capable of providing accurate external calibration elements in one direction, and for its vertical direction, the calibration result is not accurate enough. So 2D planar targets, which are the most widely-used

Table 4.1
Some feature-based multi-LRF calibration methods.

Targets	Advantages	Disadvantages
Retro-reflective targets [109]	More accurate and faster	Needs the initial parameters, intra-loop changes may not be captured
In a parking lot [112]	No artificial targets	Needs the initial parameters, require special external environment
Scanning perpendicular planes [113]	More accurate	Needs the initial parameters and a large number of observations
Two orthogonal planes [114]	Without any extra sensors or known motion information	Linear equations may degenerate due to plane poses and a relative pose.
A common planar surface [115]	Accurate, easy to perform, fast, not require specific calibration patterns	Require three LRFs
A mobile sphere [110]	Automatic and accurate	Have to move the sphere to get enough matching points, needs the initial parameters
Existing Cuboid-Shaped Corridor [116]	Require less number of observations	Needs the initial parameters
A internal corner in the room [117]	Not require specific calibration patterns	Only on 3 degree of freedom(DOF) calibration, LRFs must be set at the same plane
Trihedron [118]	Flexible, not require multiple observations or initial values of extrinsic parameters	Accuracy is not very high
A sphere [119]	Accurate and robust, long baseline and large viewpoint difference	No online calibration

calibration targets, are introduced in the calibration. Different features on the planar targets are extracted for the calibration, such as center of circles (Luo and Wu [125]), crosspoints (Yang et al. [126]), and parallel lines (Wei et al. [127]). Checkerboards are common planar targets for calibration as their corners and crossings are easily detected accurately with high flexibility (Yang et al. [126],Rufli et al. [128],Lee et al. [129]). Checkerboards allow to calculate intrinsic and extrinsic parameters for multiple cameras at the same time. Circles with various conditions are applied for calibration, including coplanar circles (Chen et al. [130]), concentric circles (Jiang and Quan [131]), coaxial circles (Colombo et al. [132]) and parallel circles (Wu et al. [133]). These targets provide planar restrictions, but for multiple cameras, the condition of simultaneous visibility is still required.

The main disadvantage of planar objects is the problem of occlusion. One of the solutions is using 3D spheres. Guan et al. [134] identify several advantages of the spheres:

1. When observed from an arbitrary direction, spheres have a similar appearance, allowing their centers to be used as feature points.
2. Finding corresponding spheres in various views is relatively easy, even in low-resolution images.
3. It is possible to calculate the distance to a specific camera if the sphere size is known.

Nevertheless, the precision of calibration is considerably affected by the correctness of ellipse fitting (Huang et al. [135]).

The above part has demonstrated feature-based multi-camera calibration methods with overlapping views. Despite this, cameras usually have no overlapping views or only a small common FOV in practical applications, such as in an advanced sensing and perception Advanced Driver-Assistance System (ADAS) system. This kind of multi-camera system is common in a mobile multi-sensor system, so now the non-overlapping problem becomes the main focus. Motion-based calibration and external measuring equipment are two ways to solve the non-overlapping calibration problem. In Table 4.2, there are additional two solutions: using large-scale targets, or using mirrors.

Large-scale targets are traditional tools for non-overlapping calibration problem. The main principle is as follows. There are several sub-targets in the large-scale target system with known positional relationships. Each camera captures only one sub-target, and then the individual external parameters are estimated. Moreover, the relationships between the sub-targets are known, which allows the external parameters to be combined in the same large-scale target frame.

The classification of large-scale targets is similar to that of the common targets which is listed in Table 4.2: 1D large-scale targets and 2D large-scale targets. 1D targets are usually combined for global calibration (Liu et al. [139], Sun et al. [140], Xie et al. [141]). It is adjustable and easy to place. However, it only allows to calibrate two cameras at one time. A planar target system is also an alternative for non-overlapping calibration (Liu et al. [142], Strauß et al. [143], Zhang et al. [144]). A 2D large-scale planar target system has high adaptability and is utilized in various environments. However, the images are generally defocused easily and calibration is not as accurate since it is generally composed of multiple sub-targets.

Mirror-based calibration is another solution for the non-overlapping problem. Reflections and mirror positions assist in obtaining extrinsic parameters. Using a plane mirror to determine external parameters requires at least three reflections of the reference object (Kumar et al. [145], Takahashi et al. [146], Fujiyama et al. [148], Mariottini et al. [149], Gluckman and Nayar [150], Xu et al. [151]). Amit Agrawal [147] proposed a new method using only one spherical mirror, but the distortion of the spherical mirror greatly affects the accuracy.

For small systems with only a few cameras, the mirror-based design is relatively simple and easy. But for large-scale measurement systems, this approach will encounter some practical difficulties. Using mirrors is an easy way to convert non-overlapping problems into overlapping calibration. However, one of the most difficult challenges is to ensure that all cameras observe the same target from different perspectives. Besides, the actual distance from the camera to the target in the mirror is twice that from the camera to the mirror. It is important to consider whether the acceptable accuracy is achievable.

4.3. Feature-based 2D LRF and camera calibration

Research has historically focused on external calibration of 2D LRFs and cameras. Some of them are summarized in Table 4.3. As mentioned in Section 2.1.2, a 2D LRF emits only a single laser beam, therefore, it is essential to build the point to line constraints in the calibration. Several studies have used V-shape target to establish the correspondence between the image and point clouds. As shown in Fig. 4.2, Wasielewski and Strauss [152] first investigated the calibration using a V-shape target. This calibration method matches the image

Table 4.2
Different feature-based multi-camera calibration methods.

Overlapping views		Year	Authors
0D Targets	Points	2005	Svoboda et al. [121]
1D Targets	1D objects composed of 3 collinear points moving around one of them	2004	Zhang [122]
	1D calibration object rotating around a known fixed point	2005	Wu et al. [123]
	1D object undergoing general rigid motions	2007	Wang and Wu [124]
2D Target	LCD projector projects structured light patterns (checkerboard)	2008	Yang et al. [126]
	Several views of the free-position planar pattern	2007	Xue et al. [136]
	A circle grid	2008	Luo and Wu [125]
	A planar target with several parallel lines	2014	Wei et al. [127]
	Depth-weighted normalized points on checkerboards	2021	Koo et al. [137]
3D Target	Spheres	2011	Wong et al. [138]
	A cube with chessboard patterns on four sides	2019	Huang et al. [135]
Non-overlapping views: no external equipment		Year	Authors
1D Large-scale Target	Using the co-linearity of points on 1D Target	2011	Liu et al. [139]
	Two 1D targets	2011	Sun et al. [140]
	A flexible target composed of two short 1D bars with equally placed light spots and one long linking pole	2013	Xie et al. [141]
2D Large-scale Target	A multi-target consist of several fixed planar sub-targets	2011	Liu et al. [142]
	Coded checkerboard	2014	Strauß et al. [143]
	A positive quadrangle, and its 5 planes are all target planes	2019	Zhang et al. [144]
Non-overlapping views: with external equipment		Year	Authors
Mirror	5 planar mirrors	2008	Kumar et al. [145]
	3 planar mirrors	2012	Takahashi et al. [146]
	A non-planar spherical mirror	2013	Agrawal [147]

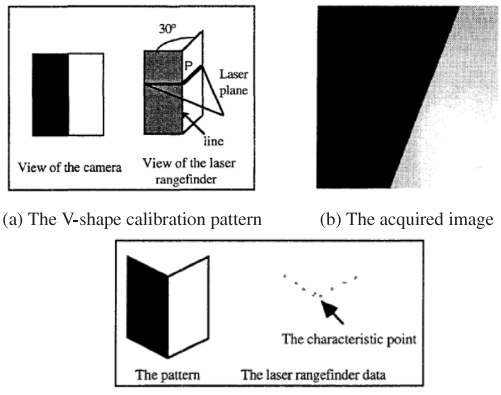

(a) The V-shape calibration pattern (b) The acquired image

(c) The acquired points

Fig. 4.2. Use V-shape target to establish the correspondence between the image and point clouds (Wasielewski and Strauss [152]).

of the line in the 3D space with the intersection to the laser plane. However, due to insufficient constraints of the point-to-line conditions, the angle between the line and the laser plane at various positions will affect the calibration result. Therefore, the point-to-line calibration requires numerous observations to obtain reliable results. Much of the research attempted to reduce the number of observations and improve the accuracy of calibration (Li et al. [153], Kwak et al. [154]). Even so, the accuracy is still insufficient.

Using point-to-plane constraints is another typical way for the external calibration. Qilong Zhang and Pless [155] solved the external parameter based on observing a planar checkerboard pattern. Over the past decade, most research in point-to-plane calibration tries to find the minimal solution (Vasconcelos et al. [157], Gomez-Ojeda et al. [158], Hu et al. [159], Dong and Isler [160]). It is known that two points determine a unique straight line on the plane. Thus, one laser beam acquired from a 2D LRF provides two practical constraints for a planar target. Qilong Zhang and Pless [155] used a 3×3 matrix to describe the transformation between the 2D LRF and the camera, therefore, there are 9 unknowns which means at least 5 observations are required to estimate the external parameter. According to Vasconcelos et al. [157], Zhang's extrinsic calibration is in general non-plausible as the iterative estimation may run into local minima. They analyzed a minimal closed-form solution from three input planes, which reduced the number of observations to a minimum of three. Some authors used multiple checkerboards to reduce the number of frames required for calibration (Hu et al. [159], Dong and Isler [160]), while some other researchers used existing geometric scene conditions to constrain the geometric positions (Gomez-Ojeda et al. [158]). Dong and Isler [160] discussed the current popular calibration targets for a 2D LRF and a camera. However, all these processes need at least three observations. The difference is only to collect the information of three planes at one time or get the data of one plane three times.

4.4. Feature-based 3D LiDAR and camera calibration

Up to now, there are many toolboxes for LiDAR and camera calibration, including Autoware (Kato et al. [161]), Apollo (Baidu [162]), "lidar and camera calibration" package (Dhall et al. [163]). The calibration targets of these mature solutions ordinarily based on the checkerboard pattern design, which is one of the most popular patterns. Compared to 2D LRFs, a 3D LiDAR emits and receives multiple laser beams, which means 3D LiDARs obtain more information, such as the normal vectors of points (Zhou and Deng [164]). 3D LiDAR and camera calibration is a 6 degree of freedom (DOF) problem with six unknowns. Similar to 2D LRF and camera calibration, each observation of the checkerboard provides three constraints. Since the calibration of multiple observations will affect accuracy, there has been an increasing amount of literature on how to increase the number of constraints acquired in a single shot in recent years. Various studies have assessed the effect of different calibration targets. Table 4.4 compares the features of some typical calibration objects. From the Table 4.4, we can see that typical characteristic include intensities, edges, normal, gradient, and the combination of several features.

In addition to estimating external parameters based on point constraints on the plane, another idea is to obtain the center of the circle

Table 4.3
Some representative 2D LRF and camera extrinsic calibration methods.

Target	Constraints	Observation	Year	Author
V-shape target	Point-to-line	at least 100	1995	Wasielewski and Strauss [152]
a planar checkerboard	Point to line	at least 5	2004	Qilong Zhang and Pless [155]
Right-angled triangular checkerboard	Point to line	at least 100	2007	Li et al. [153]
2 V-shape targets	Edge and centerline	at least 50	2011	Kwak et al. [154]
a black line on a white sheet of paper	Point to line	at least 6	2011	Naroditsky et al. [156]
Freely moving a checkerboard pattern	Point-to-line	3	2012	Vasconcelos et al. [157]
Orthogonal trihedrons (scene corners)	Line-to-plane Point-to-plane	2	2015	Gomez-Ojeda et al. [158]
Virtual trihedron (three shots of the chessboard pattern at three different times)	Point-to-Point Point-to-line	1	2016	Hu et al. [159]
2 triangular boards with a checkerboard on each triangle	Point-to-plane	1	2018	Dong and Isler [160]

Table 4.4
Some representative 3D LiDAR and camera extrinsic calibration methods.

Target	Features	Year	Author
Checkerboard	Extend from 2D to 3D LiDAR	2010	Pandey et al. [168]
	Use the weight of the normal vector uncertainty to evaluate the scan quality; Applied to both 3D and 2D LiDAR	2012	Zhou and Deng [164]
	Panoramic image; refine using the Levenberg–Marquardt method	2017	Wang et al. [169]
	educes the minimal number of observations to one by combining 3D line and plane correspondences	2018	Zhou et al. [170]
	Gaussian Mixture Model(GMM)-based intensity cluster approach	2022	Lai et al. [171]
Polygonal Planar Board	Use a low-resolution 3D LIDAR	2014	Park et al. [172]
Designed Planar Board	Two reflective crossing stripes, with an AprilTag marker placed at the intersection	2022	Grammatikopoulos et al. [173]
Nearly orthogonal multiplanar chessboard	Spatiotemporal Calibration, using Nonlinear Angular Constraints	2022	Yoon et al. [174]
Arbitrary Trihedron	Often present in structured environments, e.g., corners	2013	Gong et al. [175]
Planar targets with holes	Plane with triangular hole; 3D-3D point constraints	2012	Ha [165]
	Detect the depth difference between adjacent points under the same line to achieve edge detection; at least one observation	2014	Velas et al. [166]
Spherical	Suitable for low-resolution LiDAR data; detected from different angles	2018	Kümmerle et al. [167]
A rigid plane with a printed black ring	Simultaneous calculation of internal and external elements	2008	Fremont and Bonnifait [176]
Ordinary Box	Requires only a simple cardboard box; calibrate an arbitrary number of cameras and LiDARs; perspective-n-Point (PnP) problem	2017	Pusztai and Hajder [177], Pusztai et al. [178]
ArUco Markers	Highly reliable fiducial markers under occlusion; translation is quite accurate	2017	Dhall et al. [163]
	Using corner points of polygons as correspondence points	2021	Povendhan et al. [179]
	Calibration from multiple static scenes	2022	Zamanakos et al. [180]
Panoramic Infrastructure	Calibration of multiple cameras and 3D LiDARs from single frame.	2021	Fang et al. [181]

through edge detection using planar targets with holes (Ha [165],Velas et al. [166]) or a spherical (Kümmerle et al. [167]).

Having discussed the different calibration targets for 2D and 3D LiDARs, we will now move on to discuss the process of target-based calibration, which can be seen from Fig. 4.3. The minimal required observations for different calibration targets and applications are analyzed above. However, minimal solutions are usually unable to provide sufficiently accurate external parameters. For example, the method proposed by Li et al. [153] needs at least 100 repeated measurements to meet the accuracy specifications. Joint optimization of multiple observations may be utilized to obtain the optimal estimation, thus improving the accuracy of the measurement. There is a large volume of published studies describing fine calibration methods, including linear and non-linear least squares problems. The Levenberg–Marquardt algorithm is one of the most popular methods chosen to solve non-linear optimization problems (Wang et al. [169]).

In the early twentieth century, people manually built the constraints by selecting the 2D image features and corresponding 3D points (Zhao et al. [182],Scaramuzza et al. [183]). It is non-automatic and incredibly time-consuming. MI (Mutual Information)-based targetless calibration is able to solve the 3D–2D PnP (Perspective-n-Point) problem without considering functional relationships. Mutual Information (MI) measures the joint probability and evaluate the relationship between two datasets that are sampled simultaneously. Multi-modal image sensor data registration based on MI has been first presented in medical imaging (Hill

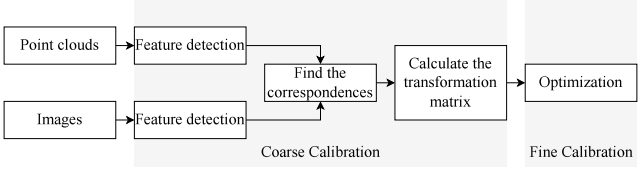

Fig. 4.3. A basic coarse to fine calibration process.

Table 4.5
Some typical features for targetless MI-based automatic calibration.

Features	Characteristics	Year	Author
Intensities	Maximizing the mutual information obtained between the sensor-measured surface intensities	2012	Pandey et al. [187]
Edges	Points with depth discontinuities correspond to edges in the image	2013	Levinson and Thrun [105]
	Edge extraction based on point cloud voxel cutting and plane fitting	2021	Yuan et al. [188]
	An adaptive voxelization technique	2022	Liu et al. [189]
Normal	The intensity of the pixels defined by the angle of the normals in the LiDAR scan	2012	Taylor and Nieto [190]
Gradient	Data registration by minimizing the misalignment of the gradients	2015	Taylor et al. [191]
Multiple features	Incorporates more features, including reflectivity, discontinuity, and surface normal	2016	Irie et al. [192]
Normalized information distance	With a view-based hidden points removal algorithm	2023	Koide et al. [193]

et al. [184]). Nowadays, MI-based calibration is becoming a common trend in computer vision and remote sensing. Table 4.5 illustrates some of the representative MI used for calibration.

Furthermore, MI has emerged as a powerful tool in airborne multi-sensor calibration and registration (Mastin et al. [185],Parmehr et al. [186]).

After obtaining the constraints from the corresponding features, the next step is to solve the PnP problem. There are many ways to solve the PnP problem, such as P3P (using three pairs of points to estimate the pose) (Gao et al. [194]), DLT (direct linear transformation), and Bundle Adjustment.

MI-based methods are automatic and accurate. However, a significant problem with these methods is the limitation of local optimization. Therefore, the initial value is necessary. Hand-eye calibration provides initial values to improve the efficiency of the algorithm, which have been discussed in Section 3.

4.5. Other feature-based multi-modal image sensor calibration

In addition to the imaging sensors discussed above, there are several other types of perceptual sensors employed in multi-modal systems. The subsequent section focuses on joint extrinsic calibration of multiple sensors and identifies two distinct types of calibration methods: the one-step target-based calibration approach and the two-step approach. Also, in this section we will discuss the calibration of airborne multi-modal sensor systems.

4.5.1. One-step target-based extrinsic calibration

Various constraints based on geometry or mutual information are applied as the conditions for multi-sensor calibration. For complicated sensor extrinsic calibration, it is crucial to design a specific target that meets the requirements of various sensors at the same time to calibrate the multi-sensor system. As shown in Fig. 4.4, Zhao et al. [195] employed a calibration board which is made of a rectangular flat board and an ArUco marker for LiDAR-ToF-Binocular calibration (Fig. 4.4(a)). Domhof et al. [196] proposed an object that is detectable by LiDAR, camera, and Radar (Fig. 4.4(b)). Besides, Peršić et al. [197] constructed another target for the LiDAR, camera and Radar joint calibration(Fig. 4.4(c)).

4.5.2. Two-step extrinsic calibration

There are extensive studies that have been conducted on the calibration of LiDAR and cameras. Hence, cameras or LiDARs are useful intermediaries for solving some complex calibration issues. Zhang et al. [198] used a monocular visual camera to assist the extrinsic calibration between a Sparse 3D LiDAR and a thermal Camera. The sensor frame diagram and two-step calibration method process are set out in Fig. 4.5.

4.5.3. Feature-based airborne multi-modal sensor calibration

Airborne platforms, such as unmanned aerial vehicles (UAVs) and manned aircraft, require precise sensor calibration for remote sensing, mapping, and defense applications. However, the calibration process for airborne platforms face unique challenges due to high-speed motion, vibration, and varying environmental conditions. Thus, feature-based calibration methods are highly desired, which offer high accuracy, robustness, and efficiency to address the challenges. Traditional calibration methods rely on using control points. In recent years, significant research efforts have been focused on calibration and localization methods that without control points (Cai et al. [199]). Active positioning algorithms based on Laser scanner (Bai et al. [200]) and Radar (Song et al. [201]) are often utilized as positioning techniques in georegistration to directly provide distance information of targets. For these methods, overlapping fields of view are a necessary condition.

5. Systematic multi-modal sensor calibration

As discussed so far, most calibration methods are based on specific pairwise combinations of sensor modes. Some recent research has focused on establishing a general calibration framework for improving the accuracy of sensor calibration across a variety of modes. Oliveira et al. [202] presented a general calibration methodology (ATOM), which is a complete framework for a calibration pipeline containing all the stages involved in the calibration process. Another calibration framework was presented by Rato et al. [203], which enables the accurate calibration of a collaborative cell containing three RGB cameras, a depth camera, and three 3D LiDARs. These frameworks, however, are not really general frameworks; the majority of frameworks provided by the research are only suitable for a limited range of applications. This area of research still requires further investigation.

The framework introduce above only explored external calibration, which specifies how the sensor has to be positioned in relation to the reference frame. Several studies have looked into combining positioning and modeling to determine the transformation matrix between the sensors as well as locate the multi-sensor system in the global coordinate system. Systematic calibration eliminates the need for a separate calibration process for each subsystem by estimating the calibration parameters simultaneously (Elseberg et al. [204]). Cucci and Matteucci [205], for example, used GPS, inertial sensors, and visual odometry to self-calibrate sensors. Cucci et al. [206] also suggested a dynamic network using bundle adjustment for the integration of image, raw inertial measurement, and GNSS observations in a tightly connected way. Multi Sensor-Fusion Extended Kalman Filter (MSF-EKF) processes delayed, relative, and absolute observations from a theoretically infinite number of distinct sensors and sensor types while allowing online sensor-suite self-calibration (Lynen et al. [207]). To integrate IMU, camera, GPS, 2D LiDAR, pressure altimeter, and magnetometer, Shen et al. [208] used a loosely coupled, derivative-free Unscented

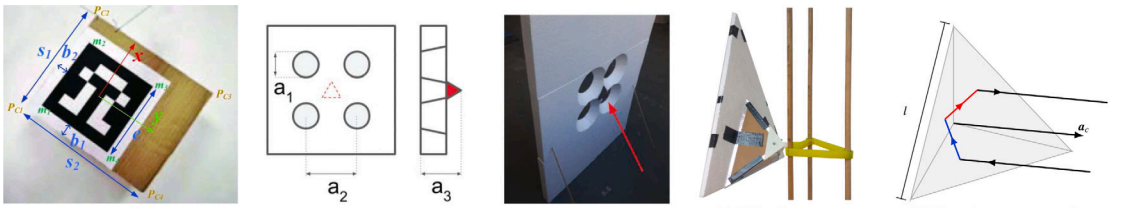

(a) Calibration target consists of a flat rectangular board and an ArUco marker (Zhao et al. [195])

(b) A frontal view drawing, a side view drawing, and an image of the back of the target. A trihedral corner reflector is indicated by a red triangle and arrow (Domhof et al. [196])

(c) An illustration of the triangular trihedral corner retroreflector and calibration target (Peršić et al. [197])

Fig. 4.4. Some examples of calibration target set-ups.

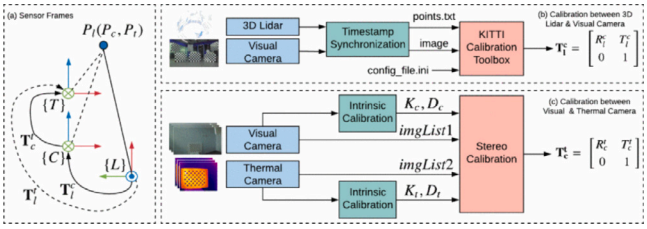

Fig. 4.5. The diagram of the sensor frames and the two-step calibration method (Zhang et al. [198]).

Kalman Filter (UKF) architecture. Recently, Lee et al. [209] developed a multi-sensor aided inertial navigation system (MINS) that uses plane patches to efficiently integrate multi-modal measurements from the IMU, camera, wheel encoder, GPS, and 3D LiDAR. Besides, based on a LiDAR/GNSS/INS-assisted structure from motion (SfM) strategy, Zhou et al. [210] generated an image-based point cloud and subsequently identified the feature correspondences between the image-based and LiDAR point clouds. A multi-sensor calibration procedure is then performed using the ICP method. Another issue that needs to be addressed for systematic online calibration is real-time performance due to excessive data volumes. A solution is to use sparse LiDAR point clouds to update and calibrate the system (Lee et al. [211]).

The necessity of time synchronization is highlighted in Section 2.2.1. Many previous research assumed that time synchronization was complete, yet time synchronization is still an important element to address in practice. Rehder et al. [212] established a general framework for the simultaneous calibration of temporal offsets and spatial transformations between numerous sensors utilizing a continuous-time state model. The temporal and spatial calibration between the IMU and camera proposed by Mair et al. [213] uses phase consistency to estimate the time offset. Using Gaussian Processes (GPs) as a means of determining moving target trajectories, Peršić et al. [214] obtained spatiotemporal calibration of moving targets. Also, some visual-inertial real-time motion estimation methods use time offset as an additional state of estimation. Accordingly, Qiu et al. [215] regards the time offset as a constant unknown value throughout the observation period and employs motion correlation analysis to calibrate heterogeneous sensors in real time.

Systematic calibration of multiple sensors is also especially critical for UAV platforms. The accuracy of registration for point clouds derived from LiDAR data and images as well as their relationship with ground truth will be greatly enhanced by estimating the external calibration parameters of LiDARs and cameras and calculating their relationship with the on-board GNSS/INS (inertial navigation system) unit simultaneously. The main procedures are mainly based on linear or planar features as discussed previously, but the data comes from different flight paths. For instance, Ravi et al. [216] used specifically designed calibration boards with highly reflective surfaces as the targets.

Finally, it should be noted that in a multi-sensor network, the calibration process can be performed through centralized or distributed approaches. Centralized approaches (Lian et al. [217], Gao et al. [218], Li et al. [219]) refer to methods that use a central processing unit to perform the calibration process, where all the sensors are connected to this unit. The unit then receives the data from all sensors, performs the calibration, and distributes the corrected data back to the sensors. On the other hand, distributed approaches (Üney et al. [220], Gao et al. [221], Gao et al. [222]) refer to methods that distribute the calibration process among the sensors themselves. Each sensor performs its own calibration, and then communicates the corrected data to the other sensors in the network. This approach reduces the need for a central processing unit, and can lead to faster and more efficient calibration. However, it also requires more coordination between the sensors to ensure that all of them are calibrated correctly. Centralized approaches are best for high-data volume, high-accuracy, and systems where sensors cannot perform calibration on their own. Distributed approaches are best for decentralized, fault-tolerant systems, and where sensors can perform calibration on their own, with limited communication bandwidth or power constraints. The choice depends on specific application and system requirements.

6. Discussion

This section covers the key factors for evaluating calibration methods in multi-modal sensor systems, including the advantages and disadvantages of each categories. The suggested calibration methods are also provided based on the specific requirements of the application. Additionally, potential research directions are highlighted based on the evaluation factors, pointing towards promising areas for future development.

6.1. Key factors for evaluation

Turning our attention to the evaluation of various calibration methods, it is important to note that accuracy alone is not the only factor that needs to be considered in the evaluation of multi-modal imaging sensor calibration. Other factors, such as efficiency, should also be evaluated in order to develop a comprehensive understanding of the strengths and limitations of each approach. Table 6.1 shows an overview of evaluations of different external calibration methods.

6.1.1. Accuracy

Accurate calibration of multi-modal sensors is critical for achieving reliable and precise measurements. However, obtaining accurate 6 degrees of freedom (DOF) parameters that define the relationship between sensors remains a challenging task. Evaluating the accuracy of calibration methods is also difficult due to the lack of standard evaluation criteria. Lack of standard evaluation criteria has led to the use of custom solutions (Guindel et al. [223]). Many of these are founded on inaccurate manual annotations (Geiger et al. [224],Nagy et al. [225]). Levinson and Thrun [105] proposed a method to detect misalignment according to the change of the objective function calculated based on the discontinuities in the scene. Kwak et al. [154] used the real LiDAR scan line on the calibration target as ground truth

Table 6.1
Evaluation of different external calibration methods.

Methods		Accuracy	Observation	Non-overlapping FoVs	Automaticity	Initial value	Robustness
Artificial feature	*Checkerboards*	High	Multiple	Not suitable	No	Require	Low
	Sphere	High	Several	Suitable	No	Require	Medium
	Others	High	Depends	Depends	Depends	Depends	Depends
Non-artificial feature	*Trihedron*	High/Medium	Several	Not suitable	Depends	Require	Medium
	Lines and planes	Medium	Multiple	Not suitable	Yes	Require	High
MI		High/Medium	Several	Not suitable	Yes	Require	Medium
Motion-based	*hand-eye calibration*	Low	Multiple	Suitable	Yes	Not require	High
Deep learning		Medium/Low	Multiple	Suitable	Yes	Not require	High

and then calculated the line alignment error and the point correspondence error. They also manually evaluated the performance through colorizing of calibrated LiDAR points. Guindel et al. [223] defined nine different calibration setups to analyze the ability of generalization of the proposed approach.

In general, there are three main factors that can impact the accuracy of multi-sensor calibration.

- Number of observations: multiple measurements are typically required to achieve acceptable accuracy.
- Overlapping fields of view: non-overlapping FoVs can make calibration more challenging.
- Robustness: calibration methods should be robust to noise and other uncertainties.

A detailed discussion of the aforementioned factors, as well as other important considerations, is presented in the following parts.

6.1.2. Observations

As discussed in Section 4.3, various studies have assessed the number of required observations in the calibration. While repeated observations are undoubtedly valuable for enhancing measurement accuracy, it is also essential to consider the minimum number of measurements required to attain an acceptable level of accuracy. This is particularly relevant when assessing the performance of various calibration methods, as some methods may require a larger number of measurements to achieve the desired level of accuracy. For example, the calibration method presented by Wasielewski and Strauss [152] depends on insufficient point-to-line constraints. Therefore, a large number of observations is required to achieve sufficient accuracy. Some researchers work on getting the calibration results in one shoot. Qilong Zhang and Pless [155] defined a 9-parameter 3×3 transformation matrix. Vasconcelos et al. [157] reduced the 9-parameter to 6-parameter to solve the 6 DOF problem. General measurement only gets 2 (2D LRF) or 3 (3D LiDAR) conditions, so for ordinary planar targets, one observation is not enough. Particular objects are designed for external calibration to achieve external parameters in one measurement, such as planar targets with holes (Velas et al. [166]), V-shape target with checkerboards pattern (Dong and Isler [160]), and Panoramic Infrastructure (Fang et al. [181]).

6.1.3. Non-overlapping FoVs

Various sensors have diverse fields of view (FoV) angles, which can lead to overlapping or non-overlapping FoVs in a multi-sensor system. The degree of FoV overlap affects the accuracy of feature correspondences and ultimately impacts the calibration accuracy. Calibration methods must take into account the FoV overlap when assessing the calibration accuracy. For calibration targets, plane targets like checkerboards have occlusion problems, requiring sensors to have a common FoV. On the other hand, 3D objects such as a sphere can be used for non-overlapping calibration because they offer consistent observation from all aspects. Moreover, both motion-based and deep learning-based calibration methods are suitable for non-overlapping calibration scenarios.

6.1.4. Robustness

In the context of calibration, robustness has two dimensions: the ability of the method to be applied in various environments, as well as its capacity to minimize calibration errors while the system is in motion. As previously discussed, target-based calibration is known for its poor robustness. The robustness of feature-based calibration without targets, on the other hand, relies heavily on the choice of features. Motion-based calibration is considered to be more robust. In cases where the environment remains stable, deep learning has proven to be an effective calibration method. However, it may not be feasible in situations where the background differs significantly.

6.1.5. Automaticity

Automated calibration refers to the absence of manual intervention in the calibration process. Target-based calibration methods do not require initial values in an automated calibration process. Thus, special-designed targets are typically required to achieve this objective. On the other hand, for targetless calibration, feature-based calibration typically employs hand-eye calibration for initial estimations, which is also classified as an automated method. Notably, deep learning-based calibration is usually considered an automated method.

6.1.6. Initial value

For feature-based calibration, providing initial values can enhance the efficiency of feature matching. However, it is possible to eliminate the need for initial parameters by employing specially designed targets or optimization methods (Owens et al. [226]). For example, circles can be detected based on their geometric features, and their centers can then be determined. In addition, many researchers utilize the results of motion-based calibration as initial values.

6.2. Applications

In the previous section, we presented several key factors for evaluating calibration methods. Table 6.2 describes the advantages and disadvantages of various calibration methods, as well as their potential application scenarios, based on the evaluation factors we have discussed.

This section further explores the significance of multi-sensor application scenarios in selecting appropriate calibration methods. Table 6.3 highlights the various fields in which multi-sensors are commonly used and includes new reviews in those respective fields, along with recommended calibration methods. The table demonstrates the widespread use of multi-modal sensor systems across various fields. As can be seen from Table 6.2 and Table 6.3, due to varying objectives, sensor types, and accuracy requirements, calibration methods employed may differ accordingly. An example of a field that requires highly accurate measurements is structural health monitoring. In such scenarios, motion-based calibration methods may not achieve the required level of precision, necessitating the use of feature-based calibration methods. In the field of autonomous driving and mapping, both high

Table 6.2
The advantage and disadvantage of different external calibration methods.

Methods		Advantages	Disadvantages	Scenarios
Artificial feature	Checkerboards	High accuracy	Require initial value, cannot be automated, not support online calibration, require overlapping FoVs	High-accuracy measurement, factory configuration of some multi-modal sensor systems.
	Sphere	High accuracy, not require overlapping FoVs	Require initial value, cannot be automated, not support online calibration	High-accuracy measurement, factory configuration of some multi-modal sensor systems.
	Other special-designed targets	High accuracy	Cannot be automated, not support online calibration	Depends on the target design, factory configuration of some multi-modal sensor systems.
Non-artificial feature	Trihedron	High/Medium accuracy	Require initial value, not fully automated, require overlapping FoVs	In structured environments
	Lines and planes	Medium accuracy, can be automated	Require initial value, require overlapping FoVs	Online calibration
MI		Can be automated	Low accuracy, require initial value, require overlapping FoVs	Online calibration
Motion-based	hand-eye calibration	Can be automated, not require initial value, not require overlapping FoVs	Low accuracy	Online calibration, provide initial values for feature-based calibration
Deep learning		Can be automated, not require initial value, not require overlapping FoVs	Low accuracy, environment consistency required	Online calibration

Table 6.3
Applications of multi-modal sensor systems and the related suggested calibration methods.

Category	Applications	Suggested methods
Industrial Automation	Robotics [227]	depends
	Manufacturing [228]	feature-based
	Structural health monitoring [229,230]	feature-based
Agriculture	Precision agriculture [231]	feature-based
	Poultry production [232]	feature-based
Transportation	Autonomous driving [233]	motion-based/targetless
	Mapping and surveying [234]	feature-based
	Smart city [235]	depends
Defense and Security	Defense [236]	depends
Healthcare	Medical imaging [237]	feature-based
	Patient monitoring [238,239]	motion-based/targetless

initial calibration accuracy and drift reduction during operation are crucial for ensuring system stability. Therefore, the use of motion-based or environment-based targetless methods for online calibration is of paramount importance.

6.3. Future research directions

Section 6.1 discusses the critical factors for evaluating these methods and Section 6.2 provides some typical applications. Drawing from these aspects, there are several insights for future research.

6.3.1. Accuracy and related factors

Most research on multi-sensor calibration has been carried out in improving accuracy. However, there is still lack of research on how to evaluate the performance of the methods because the environment of each multi-sensor system is not the same. Recently, Mishra et al. [240] evaluated three different target-based 3D LiDAR and camera calibration algorithms through error metrics such as Mean Line Re-projection Error (MLRE) and Factory Stereo Calibration Error. They also discussed their robustness to random initialization and the influence of noisy sensors. Also, some researchers are trying to improve the accuracy of calibration by developing optimization models. Kang and Doh [241] calculated the analytical gradient of the proposed cost function to enhance the accuracy of optimization. What is more, the issue of drift errors has grown in importance in light of the development of autonomous driving systems. For example, Nedevschi et al. [242] adjusted the value of six parameters automatically by online cross-calibration.

As mentioned before, a planar target will face the problem of blocking view angle in multi-sensor calibration. Therefore, some unique targets with both 3D and 2D information are designed for calibration. Bu et al. [243] invented a triangular pyramid target with checkerboard patterns on its three planes. Li et al. [244] proposes an initialization theory where cameras share a limited field of view by matching across different cameras and between two key frames using cost functions that contain inaccurate calibration parameters.

Robustness is another key factor in a multi-sensor system, especially for an online driving system. Usually, information from other sensors such as GPS or IMU (Wang et al. [245]) or from the time series increases the robustness of the system. Levinson and Thrun [105] presented that multiple frames in the time order can be utilized for the optimization. Targets of opportunity are a crucial approach for online calibration that utilizes features in the environment. Future research directions in this area include investigating the effectiveness of using multiple opportunity targets to enhance calibration reliability, studying the impact of various environmental factors (such as lighting conditions and weather) on the efficacy of targets of opportunity-based calibration methods, and exploring the potential of integrating targets of opportunity-based calibration methods with other techniques (such as feature-based methods) to improve overall accuracy and robustness.

6.3.2. Other possible research directions

Environment. Research on automatic calibration has been mostly restricted to environments with a large amount of point, line, and plane constraints, such as indoors, highways, or urban roads. Muñoz-Bañón et al. [246] presented a co-registration approach and used a Kalman Filter to improve robustness against noisy observations. To date, there has been no reliable approach for online calibration in unstructured environment, for example, country lanes or undergrounds (Ebadi et al. [247]).

Other sensors. Although there are multiple ways to calibrate a multi-sensor system that contains dense 3D LiDAR, sparse 3D LiDAR is still a popular research direction because of the relatively low price. There have been many studies on sparse 3D LiDAR calibration (Xiao et al. [248], Zhang et al. [249], An et al. [250]), but because sparse LiDAR only generates sparse point clouds, there is yet no perfect solution. In addition, there are also some studies on external calibration other than LiDAR and cameras, such as IMU-camera (Bender et al. [251]) and radar-camera (Wise et al. [252]), which is similar to LiDAR and camera calibration. Finally, several unresolved issues remain about the calibration of multiple sensors rather than two sensors.

Deep learning. Deep learning has a wide-spread popularity in various applications, including multi-sensor calibration. It is a powerful method but requires many training data and is not suitable for environments with significant feature differences. Further research is necessary to make better use of deep learning.

Simultaneous temporal and spatial calibration. Recently, an increasing number of research have begun to utilize online calibration to simultaneously calculate the parameters of spatial and temporal calibration (Li and Mourikis [253], Qin and Shen [254], Qiu et al. [215]). This is also critical in order to improve the accuracy of a multi-sensor system.

7. Conclusion

In conclusion, this paper has provided a comprehensive overview of the different external multi-modal imaging sensor calibration methods, which are widely used in various applications. This review evaluates various calibration techniques for external imaging sensors, including traditional motion-based calibration and feature-based calibration. Feature-based calibration covers target-based calibration as well as targetless approaches such as the use of features from the environment, known as target of opportunity methods. Moreover, the manuscript emphasizes the emerging research direction of systematic calibration, which is a promising area for future research. The discussion in Section 6 on the evaluation factors indicates that no approach is universally applicable, and the choice of calibration method will depend on the specific requirements of the application. Furthermore, we have highlighted some potential research directions, such as improving the capability of targetless calibration and systematic multi-modal sensor calibration. This review provides valuable insights for researchers and practitioners working in the field of multi-modal sensor systems, and that it contributes to the advancement of these systems.

CRediT authorship contribution statement

Zhouyan Qiu: Conceptualization, Investigation, Writing – original draft, Writing – review & editing, Visualization. **Joaquín Martínez-Sánchez:** Writing – review & editing, Supervision. **Pedro Arias-Sánchez:** Writing – review & editing, Supervision, Project administration. **Rabia Rashdi:** Writing – review & editing.

Declaration of competing interest

The authors declare that they have no known competing financial interests or personal relationships that could have appeared to influence the work reported in this paper.

Data availability

No data was used for the research described in the article.

Acknowledgments

We would like to express our sincere gratitude to the reviewers for their valuable feedback and constructive criticism, which significantly contributed to improving the quality of this review paper.

This project has received funding from the European Union's Horizon 2020 research and innovation programme under the Marie Skłodowska-Curie grant agreement No 860370.

This work has been supported by Gobierno de España: Ministerio de Ciencia, Innovació n y Universidades through the Grant PID2019-108816RB-I00 funded by MCIN/AEI/ 10.13039/501100011033.

Funding for open access charge: Universidade de Vigo/CISUG.

References

[1] J.K. Hackett, M. Shah, Multi-sensor fusion: A perspective, in: Proceedings., IEEE International Conference on Robotics and Automation, IEEE, 1990, pp. 1324–1330.

[2] L. Luo, X. Wang, H. Guo, R. Lasaponara, X. Zong, N. Masini, G. Wang, P. Shi, H. Khatteli, F. Chen, et al., Airborne and spaceborne remote sensing for archaeological and cultural heritage applications: A review of the century (1907–2017), Remote Sens. Environ. 232 (2019) 111280.

[3] K. Nagla, M. Uddin, D. Singh, Multisensor data fusion and integration for mobile robots: A review, IAES Int. J. Robot. Autom. 3 (2) (2014) 131.

[4] N. Van Dinh, G.-W. Kim, Multi-sensor fusion towards VINS: A concise tutorial, survey, framework and challenges, in: 2020 IEEE International Conference on Big Data and Smart Computing, BigComp, IEEE, 2020, pp. 459–462.

[5] M. Soilán, A. Sánchez-Rodríguez, P. del Río-Barral, C. Perez-Collazo, P. Arias, B. Riveiro, Review of laser scanning technologies and their applications for road and railway infrastructure monitoring, Infrastructures 4 (4) (2019) 58.

[6] R. Rashdi, J. Martínez-Sánchez, P. Arias, Z. Qiu, Scanning technologies to building information modelling: A review, Infrastructures 7 (4) (2022) http://dx.doi.org/10.3390/infrastructures7040049, URL: https://www.mdpi.com/2412-3811/7/4/49.

[7] S. Trubia, A. Severino, S. Curto, F. Arena, G. Pau, Smart roads: An overview of what future mobility will look like, Infrastructures 5 (12) (2020) http://dx.doi.org/10.3390/infrastructures5120107, URL: https://www.mdpi.com/2412-3811/5/12/107.

[8] D.L. Hall, J. Llinas, An introduction to multisensor data fusion, Proc. IEEE 85 (1) (1997) 6–23, http://dx.doi.org/10.1109/5.554205.

[9] P. Kumar, H. Gauba, P.P. Roy, D.P. Dogra, Coupled HMM-based multi-sensor data fusion for sign language recognition, Pattern Recognit. Lett. 86 (2017) 1–8, http://dx.doi.org/10.1016/j.patrec.2016.12.004.

[10] J. Kummerle, T. Kuhner, Unified intrinsic and extrinsic camera and LiDAR calibration under uncertainties, in: Proceedings - IEEE International Conference on Robotics and Automation, Institute of Electrical and Electronics Engineers Inc., 2020, pp. 6028–6034, http://dx.doi.org/10.1109/ICRA40945.2020.9197496.

[11] M. Pollefeys, R. Koch, L. Van Gool, Self-calibration and metric reconstruction inspite of varying and unknown intrinsic camera parameters, Int. J. Comput. Vis. 32 (1) (1999) 7–25, http://dx.doi.org/10.1023/A:1008109111715, URL: https://link.springer.com/article/10.1023/A:1008109111715.

[12] J. Skaloud, D. Lichti, Rigorous approach to bore-sight self-calibration in airborne laser scanning, ISPRS J. Photogramm. Remote Sens. 61 (1) (2006) 47–59, http://dx.doi.org/10.1016/j.isprsjprs.2006.07.003.

[13] H. Brauner, Kinematik und Quaternionen. (Mathematische Monographien), Zamm-Z. Angew. Math. Mech. 42 (1962) 366–367.

[14] J. O'Rourke, Computer Graphics. Algorithms Frequently Asked Questions, Smith College, Northampton USA, 2002.

[15] H. Caesar, V. Bankiti, A.H. Lang, S. Vora, V.E. Liong, Q. Xu, A. Krishnan, Y. Pan, G. Baldan, O. Beijbom, nuscenes: A multimodal dataset for autonomous driving, in: Proceedings of the IEEE/CVF Conference on Computer Vision and Pattern Recognition, 2020, pp. 11621–11631.

[16] A. Bonarini, W. Burgard, G. Fontana, M. Matteucci, D.G. Sorrenti, J.D. Tardos, Rawseeds: Robotics advancement through web-publishing of sensorial and elaborated extensive data sets, in: Proceedings of IROS, Vol. 6, 2006, p. 93.

[17] A.Z. Zhu, D. Thakur, T. Özaslan, et al., The multivehicle stereo event camera dataset: An event camera dataset for 3D perception, IEEE Robot. Autom. Lett. 3 (3) (2018) 2032–2039, http://dx.doi.org/10.1109/LRA.2018.2800793.

[18] M. Pitropov, D.E. Garcia, J. Rebello, M. Smart, C. Wang, K. Czarnecki, S. Waslander, Canadian adverse driving conditions dataset, Int. J. Robot. Res. 40 (4–5) (2021) 681–690.

[19] A. Geiger, P. Lenz, C. Stiller, R. Urtasun, Vision meets robotics: The KITTI dataset, Int. J. Robot. Res. 32 (11) (2013) 1231–1237, http://dx.doi.org/10.1177/0278364913491297.

[20] D. Feng, L. Rosenbaum, C. Gläser, F. Timm, K. Dietmayer, Can we trust you? On calibration of a probabilistic object detector for autonomous driving, 2019, CoRR abs/1909.12358 URL: http://arxiv.org/abs/1909.12358.

[21] J. Jiang, P. Xue, S. Chen, Z. Liu, X. Zhang, N. Zheng, Line feature based extrinsic calibration of LiDAR and camera, in: 2018 IEEE International Conference on Vehicular Electronics and Safety, ICVES, IEEE, 2018, pp. 1–6, http://dx.doi.org/10.1109/ICVES.2018.8519493, URL: https://ieeexplore.ieee.org/document/8519493/.

[22] J. Houston, G. Zuidhof, L. Bergamini, Y. Ye, L. Chen, A. Jain, S. Omari, V. Iglovikov, P. Ondruska, One thousand and one hours: Self-driving motion prediction dataset, in: Conference on Robot Learning, PMLR, 2021, pp. 409–418.

[23] D. Barnes, M. Gadd, P. Murcutt, P. Newman, I. Posner, The Oxford radar RobotCar dataset: A radar extension to the Oxford RobotCar dataset, in: Proceedings - IEEE International Conference on Robotics and Automation, Institute of Electrical and Electronics Engineers Inc., 2020, pp. 6433–6438, http://dx.doi.org/10.1109/ICRA40945.2020.9196884.

[24] Y. Choi, N. Kim, et al., KAIST multi-spectral day/night data set for autonomous and assisted driving, IEEE Trans. Intell. Transp. Syst. 19 (2018) 1–15, http://dx.doi.org/10.1109/TITS.2018.2791533.

[25] S. Yogamani, C. Hughes, J. Horgan, G. Sistu, P. Varley, D. O'Dea, M. Uricár, S. Milz, M. Simon, K. Amende, et al., Woodscape: A multi-task, multi-camera fisheye dataset for autonomous driving, in: Proceedings of the IEEE/CVF International Conference on Computer Vision, 2019, pp. 9308–9318.

[26] A.S. Huang, M. Antone, E. Olson, et al., A high-rate, heterogeneous data set from the DARPA urban challenge, Int. J. Robot. Res. 29 (13) (2010) 1595–1601, http://dx.doi.org/10.1177/0278364910384295.

[27] R. Huitl, G. Schroth, S. Hilsenbeck, F. Schweiger, E. Steinbach, TUMindoor: An extensive image and point cloud dataset for visual indoor localization and mapping, in: 2012 19th IEEE International Conference on Image Processing, IEEE, 2012, pp. 1773–1776.

[28] J.-L. Blanco, F.-A. Moreno, J. Gonzalez-Jimenez, The Málaga urban dataset: High-rate stereo and LiDARs in a realistic urban scenario, Int. J. Robot. Res. 33 (2) (2014) 207–214, http://dx.doi.org/10.1177/0278364913507326, URL: http://www.mrpt.org/MalagaUrbanDataset.

[29] N. Carlevaris-Bianco, A.K. Ushani, R.M. Eustice, University of Michigan north campus long-term vision and LiDAR dataset, Int. J. Robot. Res. 35 (9) (2016) 1023–1035.

[30] M. Burri, J. Nikolic, P. Gohl, T. Schneider, J. Rehder, S. Omari, M.W. Achtelik, R. Siegwart, The EuRoC micro aerial vehicle datasets, Int. J. Robot. Res. 35 (10) (2016) 1157–1163.

[31] S. Urban, B. Jutzi, LaFiDa—A laserscanner multi-fisheye camera dataset, J. Imaging 3 (1) (2017) 5.

[32] D. Schubert, T. Goll, N. Demmel, V. Usenko, J. Stückler, D. Cremers, The TUM VI benchmark for evaluating visual-inertial odometry, in: 2018 IEEE/RSJ International Conference on Intelligent Robots and Systems, IROS, IEEE, 2018, pp. 1680–1687.

[33] V. Ramanishka, Y.-T. Chen, T. Misu, K. Saenko, Toward driving scene understanding: A dataset for learning driver behavior and causal reasoning, in: 2018 IEEE/CVF Conference on Computer Vision and Pattern Recognition, IEEE, 2018, pp. 7699–7707, http://dx.doi.org/10.1109/CVPR.2018.00803, URL: https://ieeexplore.ieee.org/document/8578901/.

[34] A. Ligocki, A. Jelinek, L. Zalud, Brno urban dataset-the new data for self-driving agents and mapping tasks, in: 2020 IEEE International Conference on Robotics and Automation, ICRA, IEEE, 2020, pp. 3284–3290.

[35] J. Delmerico, T. Cieslewski, H. Rebecq, M. Faessler, D. Scaramuzza, Are we ready for autonomous drone racing? the UZH-FPV drone racing dataset, in: 2019 International Conference on Robotics and Automation, ICRA, IEEE, 2019, pp. 6713–6719.

[36] G. Marin, G. Agresti, L. Minto, P. Zanuttigh, A multi-camera dataset for depth estimation in an indoor scenario, Data Brief 27 (2019) 104619.

[37] X. Huang, P. Wang, X. Cheng, D. Zhou, Q. Geng, R. Yang, The apolloscape open dataset for autonomous driving and its application, IEEE Trans. Pattern Anal. Mach. Intell. 42 (10) (2019) 2702–2719.

[38] M.-F. Chang, D. Ramanan, J. Hays, J. Lambert, P. Sangkloy, J. Singh, S. Bak, A. Hartnett, D. Wang, P. Carr, et al., Argoverse: 3D tracking and forecasting with rich maps, in: 2019 IEEE/CVF Conference on Computer Vision and Pattern Recognition, CVPR, IEEE, 2019, pp. 8740–8749, http://dx.doi.org/10.1109/CVPR.2019.00895, URL: https://ieeexplore.ieee.org/document/8953693/.

[39] P. Sun, H. Kretzschmar, X. Dotiwalla, et al., Scalability in perception for autonomous driving: Waymo open dataset, in: Proceedings of the IEEE/CVF Conference on Computer Vision and Pattern Recognition, 2020, pp. 2446–2454.

[40] W. Wen, Y. Zhou, G. Zhang, S. Fahandezh-Saadi, X. Bai, W. Zhan, M. Tomizuka, L.-T. Hsu, Urbanloco: A full sensor suite dataset for mapping and localization in urban scenes, in: 2020 IEEE International Conference on Robotics and Automation, ICRA, IEEE, 2020, pp. 2310–2316.

[41] J. Martinez, S. Doubov, J. Fan, S. Wang, G. Máttyus, R. Urtasun, et al., Pit30m: A benchmark for global localization in the age of self-driving cars, in: 2020 IEEE/RSJ International Conference on Intelligent Robots and Systems, IROS, IEEE, 2020, pp. 4477–4484.

[42] Q. She, F. Feng, X. Hao, Q. Yang, C. Lan, V. Lomonaco, X. Shi, Z. Wang, Y. Guo, Y. Zhang, et al., OpenLORIS-Object: A robotic vision dataset and benchmark for lifelong deep learning, in: 2020 IEEE International Conference on Robotics and Automation, ICRA, IEEE, 2020, pp. 4767–4773.

[43] J. Geyer, Y. Kassahun, M. Mahmudi, X. Ricou, R. Durgesh, A.S. Chung, L. Hauswald, V.H. Pham, M. Mühlegg, S. Dorn, et al., A2D2: Audi autonomous driving dataset, 2020, arXiv preprint arXiv:2004.06320.

[44] Q.-H. Pham, P. Sevestre, R.S. Pahwa, H. Zhan, C.H. Pang, Y. Chen, A. Mustafa, V. Chandrasekhar, J. Lin, A*3D dataset: Towards autonomous driving in challenging environments, in: 2020 IEEE International Conference on Robotics and Automation, ICRA, IEEE, 2020, pp. 2267–2273, http://dx.doi.org/10.1109/ICRA40945.2020.9197385, URL: https://ieeexplore.ieee.org/document/9197385/.

[45] M. Cordts, M. Omran, S. Ramos, T. Rehfeld, M. Enzweiler, R. Benenson, U. Franke, S. Roth, B. Schiele, The cityscapes dataset for semantic urban scene understanding, in: 2016 IEEE Conference on Computer Vision and Pattern Recognition, CVPR, IEEE, 2016, pp. 3213–3223, http://dx.doi.org/10.1109/CVPR.2016.350, URL: http://ieeexplore.ieee.org/document/7780719/.

[46] R. Kesten, M. Usman, J. Houston, T. Pandya, K. Nadhamuni, A. Ferreira, M. Yuan, B. Low, A. Jain, P. Ondruska, S. Omari, S. Shah, A. Kulkarni, A. Kazakova, C. Tao, L. Platinsky, W. Jiang, V. Shet, Level 5 perception dataset 2020, 2019, https://level-5.global/level5/data/.

[47] P. Xiao, Z. Shao, S. Hao, Z. Zhang, X. Chai, J. Jiao, Z. Li, J. Wu, K. Sun, K. Jiang, et al., Pandaset: Advanced sensor suite dataset for autonomous driving, in: 2021 IEEE International Intelligent Transportation Systems Conference, ITSC, IEEE, 2021, pp. 3095–3101.

[48] M. Liao, F. Lu, D. Zhou, S. Zhang, W. Li, R. Yang, Dvi: Depth guided video inpainting for autonomous driving, in: European Conference on Computer Vision, Springer, 2020, pp. 1–17.

[49] Y. Cheng, M. Jiang, J. Zhu, Y. Liu, Are we ready for unmanned surface vehicles in inland waterways? The USVinland multisensor dataset and benchmark, IEEE Robot. Autom. Lett. 6 (2) (2021) 3964–3970.

[50] S. Ghosh, N. Das, P. Sarkar, M. Nasipuri, JU-VNT: A multi-spectral dataset of indoor object recognition using visible, near-infrared and thermal spectrum, Multimedia Tools Appl. (2021) 1–20, http://dx.doi.org/10.1007/s11042-020-10302-z.

[51] N. Zhu, M. Ortiz, V. Renaudin, C. Ichard, S. Ricou, Dataset of the intermediate competition in challenge MALIN: Indoor–Outdoor inertial navigation system data for pedestrian and vehicle with high accuracy references in a context of firefighter scenario, Data Brief 34 (2021) 106626, http://dx.doi.org/10.1016/j.dib.2020.106626, URL: https://www.sciencedirect.com/science/article/pii/S2352340920315067.

[52] D. Lee, S. Ryu, S. Yeon, Y. Lee, D. Kim, C. Han, Y. Cabon, P. Weinzaepfel, N. Guérin, G. Csurka, et al., Large-scale localization datasets in crowded indoor spaces, in: Proceedings of the IEEE/CVF Conference on Computer Vision and Pattern Recognition, 2021, pp. 3227–3236.

[53] Y. Wang, G. Wang, H.-M. Hsu, H. Liu, J.-N. Hwang, Rethinking of radar's role: A camera-radar dataset and systematic annotator via coordinate alignment, in: Proceedings of the IEEE/CVF Conference on Computer Vision and Pattern Recognition, 2021, pp. 2815–2824.

[54] O. Schumann, M. Hahn, N. Scheiner, F. Weishaupt, J.F. Tilly, J. Dickmann, C. Wöhler, RadarScenes: A real-world radar point cloud data set for automotive applications, in: 2021 IEEE 24th International Conference on Information Fusion, FUSION, IEEE, 2021, pp. 1–8.

[55] M. Gehrig, W. Aarents, D. Gehrig, D. Scaramuzza, Dsec: A stereo event camera dataset for driving scenarios, IEEE Robot. Autom. Lett. 6 (3) (2021) 4947–4954.

[56] H.E. Keen, Q.H. Jan, K. Berns, Drive on pedestrian walk. TUK campus dataset, in: 2021 IEEE/RSJ International Conference on Intelligent Robots and Systems, IROS, IEEE, 2021, pp. 3822–3828.

[57] J. Yin, A. Li, T. Li, W. Yu, D. Zou, M2dgr: A multi-sensor and multi-scenario slam dataset for ground robots, IEEE Robot. Autom. Lett. 7 (2) (2021) 2266–2273.

[58] A. Kurup, J. Bos, DSOR: A scalable statistical filter for removing falling snow from LiDAR point clouds in severe winter weather, 2021, arXiv preprint arXiv:2109.07078.

[59] J. Mao, M. Niu, C. Jiang, H. Liang, J. Chen, X. Liang, Y. Li, C. Ye, W. Zhang, Z. Li, et al., One million scenes for autonomous driving: Once dataset, 2021, arXiv preprint arXiv:2106.11037.

[60] S. Klenk, J. Chui, N. Demmel, D. Cremers, TUM-VIE: The TUM stereo visual-inertial event dataset, in: 2021 IEEE/RSJ International Conference on Intelligent Robots and Systems, IROS, IEEE, 2021, pp. 8601–8608.

[61] P. Schneider, Y. Anisimov, R. Islam, B. Mirbach, J. Rambach, D. Stricker, F. Grandidier, TIMo—A dataset for indoor building monitoring with a time-of-flight camera, Sensors 22 (11) (2022) 3992.

[62] P. Testolina, F. Barbato, U. Michieli, M. Giordani, P. Zanuttigh, M. Zorzi, SELMA: Semantic large-scale multimodal acquisitions in variable weather, daytime and viewpoints, 2022, arXiv preprint arXiv:2204.09788.

[63] X. Ye, M. Shu, H. Li, Y. Shi, Y. Li, G. Wang, X. Tan, E. Ding, Rope3D: The roadside perception dataset for autonomous driving and monocular 3D object detection task, in: Proceedings of the IEEE/CVF Conference on Computer Vision and Pattern Recognition, 2022, pp. 21341–21350.

[64] B. Wilson, W. Qi, T. Agarwal, J. Lambert, J. Singh, S. Khandelwal, B. Pan, R. Kumar, A. Hartnett, J.K. Pontes, et al., Argoverse 2: Next generation datasets for self-driving perception and forecasting, 2023, arXiv preprint arXiv:2301.00493.

[65] H. Horenstein, Black and White Photography, Little, Brown, 2005, URL: http://archive.org/details/blackwhitephotog00hore_0.

[66] R. Kingslake, A History of the Photographic Lens, Elsevier Science, 1989, URL: https://books.google.es/books?id=IaBXn06OlWsC.

[67] G. Agresti, L. Minto, G. Marin, P. Zanuttigh, Stereo and ToF data fusion by learning from synthetic data, Inf. Fusion 49 (2019) 161–173.

[68] S. Yogamani, C. Hughes, J. Horgan, G. Sistu, P. Varley, D. O'Dea, M. Uricár, S. Milz, M. Simon, K. Amende, et al., Woodscape: A multi-task, multi-camera fisheye dataset for autonomous driving, in: Proceedings of the IEEE/CVF International Conference on Computer Vision, 2019, pp. 9308–9318.

[69] R. Horaud, R. Mohr, B. Lorecki, On single-scanline camera calibration, IEEE Trans. Robot. Autom. 9 (1) (1993) 71–75.

[70] D.D. Li, G. Wen, S. Qiu, Cross-ratio–based line scan camera calibration using a planar pattern, Opt. Eng. 55 (1) (2016) 014104.

[71] B. Sun, J. Zhu, L. Yang, Y. Guo, J. Lin, Stereo line-scan sensor calibration for 3D shape measurement, Appl. Opt. 56 (28) (2017) 7905–7914.

[72] J. Draréni, S. Roy, P. Sturm, Plane-based calibration for linear cameras, Int. J. Comput. Vis. 91 (2) (2011) 146–156.

[73] B. Hui, G. Wen, P. Zhang, D. Li, A novel line scan camera calibration technique with an auxiliary frame camera, IEEE Trans. Instrum. Meas. 62 (9) (2013) 2567–2575.

[74] S. Donné, H. Luong, S. Dhondt, N. Wuyts, D. Inzé, B. Goossens, W. Philips, Robust plane-based calibration for linear cameras, in: 2017 IEEE International Conference on Image Processing, ICIP, IEEE, 2017, pp. 36–40.

[75] W. Stone, M. Juberts, N. Dagalakis, J.S. Jr., J. Gorman, Performance Analysis of Next-Generation LADAR for Manufacturing, Construction, and Mobility, NIST Interagency/Internal Report (NISTIR), National Institute of Standards and Technology, Gaithersburg, MD, 2004, http://dx.doi.org/10.6028/NIST.IR.7117, URL: https://tsapps.nist.gov/publication/get_pdf.cfm?pub_id=822493.

[76] S.W. Smith, CHAPTER 1 - The breadth and depth of DSP, in: S.W. Smith (Ed.), Digital Signal Processing, Newnes, Boston, 2003, pp. 1–10, http://dx.doi.org/10.1016/B978-0-7506-7444-7/50038-8, URL: https://www.sciencedirect.com/science/article/pii/B9780750674447500388.

[77] H. Hu, J. Wu, Z. Xiong, A soft time synchronization framework for multi-sensors in autonomous localization and navigation, in: IEEE/ASME International Conference on Advanced Intelligent Mechatronics, Vol. 2018-July, AIM, Institute of Electrical and Electronics Engineers Inc., 2018, pp. 694–699, http://dx.doi.org/10.1109/AIM.2018.8452384, URL: https://ieeexplore.ieee.org/document/8452384/.

[78] W.D. Blair, T.R. Rice, A.T. Alouani, P. Xia, Asynchronous data fusion for target tracking with a multitasking radar and optical sensor, in: Acquisition, Tracking, and Pointing V, Vol. 1482, International Society for Optics and Photonics, 1991, pp. 234–245.

[79] G. Huang, A.Y. Zomaya, F.C. Delicato, P.F. Pires, Long term and large scale time synchronization in wireless sensor networks, Comput. Commun. 37 (2014) 77–91.

[80] J. Brownlee, Introduction to Time Series Forecasting with Python: How to Prepare Data and Develop Models to Predict the Future, Machine Learning Mastery, 2017.

[81] E. Olson, A passive solution to the sensor synchronization problem, in: 2010 IEEE/RSJ International Conference on Intelligent Robots and Systems, IEEE, 2010, pp. 1059–1064.

[82] J. Kelly, N. Roy, G.S. Sukhatme, Determining the time delay between inertial and visual sensor measurements, IEEE Trans. Robot. 30 (6) (2014) 1514–1523.

[83] S. Du, H.A. Lauterbach, X. Li, G.G. Demisse, D. Borrmann, A. Nüchter, Curvefusion—A method for combining estimated trajectories with applications to SLAM and time-calibration, Sensors 20 (23) (2020) 6918.

[84] W. Liu, Z. Li, S. Sun, H. Du, M.A. Sotelo, A novel motion-based online temporal calibration method for multi-rate sensors fusion, Inf. Fusion 88 (2022) 59–77.

[85] J.J. Gibson, The Perception of the Visual World, Houghton Mifflin, 1950.

[86] F. Raudies, H. Neumann, A review and evaluation of methods estimating ego-motion, Comput. Vis. Image Underst. 116 (5) (2012) 606–633.

[87] S. Hong, H. Ko, J. Kim, VICP: Velocity updating iterative closest point algorithm, in: 2010 IEEE International Conference on Robotics and Automation, IEEE, 2010, pp. 1893–1898.

[88] T. Liu, A.W. Moore, A.G. Gray, K. Yang, An investigation of practical approximate nearest neighbor algorithms, in: NIPS, Vol. 12, Citeseer, 2004, p. 2004.

[89] Y. Balazadegan Sarvrood, S. Hosseinyalamdary, Y. Gao, Visual-LiDAR odometry aided by reduced IMU, ISPRS Int. J. Geo-Inf. 5 (1) (2016) 3.

[90] G. Yang, Y. Wang, J. Zhi, W. Liu, Y. Shao, P. Peng, A review of visual odometry in SLAM techniques, in: 2020 International Conference on Artificial Intelligence and Electromechanical Automation, AIEA, IEEE, 2020, pp. 332–336.

[91] R. Mur-Artal, J.M.M. Montiel, J.D. Tardos, ORB-SLAM: A versatile and accurate monocular SLAM system, IEEE Trans. Robot. 31 (5) (2015) 1147–1163.

[92] J. Zhang, S. Singh, LOAM: LiDAR odometry and mapping in real-time, in: Robotics: Science and Systems, 2014, pp. 1–9, http://dx.doi.org/10.15607/RSS.2014.X.007.

[93] C. Kerl, J. Sturm, D. Cremers, Dense visual SLAM for RGB-D cameras, in: 2013 IEEE/RSJ International Conference on Intelligent Robots and Systems, IEEE, 2013, pp. 2100–2106.

[94] J. Peng, Y. Shao, N. Sang, C. Gao, Joint image deblurring and matching with feature-based sparse representation prior, Pattern Recognit. 103 (2020) 107300.

[95] S. Har-Noy, E. Martinez, T.Q. Nguyen, Filter banks for improved LCD motion, Signal Process., Image Commun. 25 (1) (2010) 1–9.

[96] F. Couzinié-Devy, J. Sun, K. Alahari, J. Ponce, Learning to estimate and remove non-uniform image blur, in: 2013 IEEE Conference on Computer Vision and Pattern Recognition, 2013, pp. 1075–1082, http://dx.doi.org/10.1109/CVPR.2013.143.

[97] A.M. Deshpande, S. Patnaik, Single image motion deblurring: An accurate PSF estimation and ringing reduction, Optik 125 (14) (2014) 3612–3618.

[98] S. Anderson, T.D. Barfoot, Towards relative continuous-time SLAM, in: 2013 IEEE International Conference on Robotics and Automation, IEEE, 2013, pp. 1033–1040.

[99] A. Patron-Perez, S. Lovegrove, G. Sibley, A spline-based trajectory representation for sensor fusion and rolling shutter cameras, Int. J. Comput. Vis. 113 (3) (2015) 208–219.

[100] J. Huai, Y. Zhuang, Y. Lin, G. Jozkow, Q. Yuan, D. Chen, Continuous-time spatiotemporal calibration of a rolling shutter camera-IMU system, IEEE Sens. J. 22 (8) (2022) 7920–7930, http://dx.doi.org/10.1109/JSEN.2022.3152572.

[101] R. Horaud, F. Dornaika, Hand-eye calibration, Int. J. Robot. Res. 14 (3) (1995) 195–210, http://dx.doi.org/10.1177/027836499501400301.

[102] Z. Taylor, J. Nieto, Motion-based calibration of multimodal sensor extrinsics and timing offset estimation, IEEE Trans. Robot. 32 (5) (2016) 1215–1229.

[103] R. Ishikawa, T. Oishi, K. Ikeuchi, LiDAR and camera calibration using motions estimated by sensor fusion odometry, in: 2018 IEEE/RSJ International Conference on Intelligent Robots and Systems, IROS, IEEE, 2018, pp. 7342–7349.

[104] P. Moghadam, M. Bosse, R. Zlot, Line-based extrinsic calibration of range and image sensors, in: 2013 IEEE International Conference on Robotics and Automation, IEEE, 2013, pp. 3685–3691.

[105] J. Levinson, S. Thrun, Automatic online calibration of cameras and lasers, in: Robotics: Science and Systems, Vol. 2, Citeseer, 2013, p. 7.

[106] C. Rodríguez-Garavito, A. Ponz, F. García, D. Martín, A. de la Escalera, J.M. Armingol, Automatic laser and camera extrinsic calibration for data fusion using road plane, in: 17th International Conference on Information Fusion, FUSION, IEEE, 2014, pp. 1–6.

[107] Y. Han, Y. Liu, D. Paz, H. Christensen, Auto-calibration method using stop signs for urban autonomous driving applications, in: 2021 IEEE International Conference on Robotics and Automation, ICRA, IEEE, 2021, pp. 13179–13185.

[108] X. Liu, F. Zhang, Extrinsic calibration of multiple LiDARs of small fov in targetless environments, IEEE Robot. Autom. Lett. 6 (2) (2021) 2036–2043.

[109] C. Gao, J.R. Spletzer, On-line calibration of multiple LIDARs on a mobile vehicle platform, in: 2010 IEEE International Conference on Robotics and Automation, 2010, http://dx.doi.org/10.1109/robot.2010.5509880.

[110] S. Chen, J. Liu, T. Wu, et al., Extrinsic calibration of 2D laser rangefinders based on a mobile sphere, Remote Sens. 10 (2018) 1176, http://dx.doi.org/10.3390/rs10081176.

[111] P. Chen, W. Shi, S. Bao, M. Wang, W. Fan, H. Xiang, Low-drift odometry, mapping and ground segmentation using a backpack LiDAR system, IEEE Robot. Autom. Lett. 6 (4) (2021) 7285–7292.

[112] M. He, H. Zhao, J. Cui, H. Zha, Calibration method for multiple 2D LIDARs system, in: 2014 IEEE International Conference on Robotics and Automation, ICRA, 2014, pp. 3034–3041, http://dx.doi.org/10.1109/ICRA.2014.6907296.

[113] E. Fernández-Moral, J. González-Jiménez, V. Arévalo, Extrinsic calibration of 2D laser rangefinders from perpendicular plane observations, Int. J. Robot. Res. 34 (11) (2015) 1401–1417, http://dx.doi.org/10.1177/0278364915580683.

[114] D. Choi, Y. Bok, J. Kim, I.S. Kweon, Extrinsic calibration of 2-D LiDARs using two orthogonal planes, IEEE Trans. Robot. 32 (1) (2016) 83–98, http://dx.doi.org/10.1109/TRO.2015.2502860.

[115] E. Fernández-Moral, V. Arévalo, J. González-Jiménez, Extrinsic calibration of a set of 2D laser rangefinders, in: 2015 IEEE International Conference on Robotics and Automation, ICRA, 2015, pp. 2098–2104, http://dx.doi.org/10.1109/ICRA.2015.7139475.

[116] D. Yin, J. Liu, T. Wu, K. Liu, J. Hyyppä, R. Chen, Extrinsic calibration of 2D laser rangefinders using an existing cuboid-shaped corridor as the reference, Sensors 18 (12) (2018) http://dx.doi.org/10.3390/s18124371, URL: https://www.mdpi.com/1424-8220/18/12/4371.

[117] T. Song, B.-G. Wei, S. Guo, J.-T. Peng, D.-X. Han, A calibration method of dual two-dimensional laser range finders for mobile manipulator, Int. J. Adv. Robot. Syst. 16 (5) (2019) 1729881419876783, http://dx.doi.org/10.1177/1729881419876783.

[118] F. Zhu, Y. Huang, Z. Tian, Y. Ma, Extrinsic calibration of multiple two-dimensional laser rangefinders based on a trihedron, Sensors 20 (7) (2020) http://dx.doi.org/10.3390/s20071837, URL: https://www.mdpi.com/1424-8220/20/7/1837.

[119] J. Zhang, Q. Lyu, G. Peng, Z. Wu, Q. Yan, D. Wang, LB-L2L-Calib: Accurate and robust extrinsic calibration for multiple 3D LiDARs with long baseline and large viewpoint difference, in: 2022 International Conference on Robotics and Automation, ICRA, IEEE, 2022, pp. 926–932, http://dx.doi.org/10.1109/ICRA46639.2022.9812062.

[120] K. Schenk, A. Kolarow, M. Eisenbach, K. Debes, H. Gross, Automatic calibration of a stationary network of laser range finders by matching movement trajectories, in: 2012 IEEE/RSJ International Conference on Intelligent Robots and Systems, 2012, pp. 431–437, http://dx.doi.org/10.1109/IROS.2012.6385620.

[121] T. Svoboda, D. Martinec, T. Pajdla, A convenient multicamera self-calibration for virtual environments, Presence: Teleoperators Virtual Environ. 14 (4) (2005) 407–422, http://dx.doi.org/10.1162/105474605774785325.

[122] Z. Zhang, Camera calibration with one-dimensional objects, IEEE Trans. Pattern Anal. Mach. Intell. 26 (7) (2004) 892–899, http://dx.doi.org/10.1109/TPAMI.2004.21.

[123] F. Wu, Z. Hu, H. Zhu, Camera calibration with moving one-dimensional objects, Pattern Recognit. 38 (5) (2005) 755–765.

[124] L. Wang, F.-c. Wu, Multi-camera calibration based on ID calibration object, Acta Automat. Sinica 33 (3) (2007) 225.

[125] P.-F. Luo, J. Wu, Easy calibration technique for stereo vision using a circle grid, Opt. Eng. - OPT ENG 47 (2008) http://dx.doi.org/10.1117/1.2897237.

[126] R. Yang, S. Cheng, Y. Chen, Flexible and accurate implementation of a binocular structured light system, Opt. Lasers Eng. 46 (5) (2008) 373–379, http://dx.doi.org/10.1016/j.optlaseng.2007.12.008, URL: https://www.sciencedirect.com/science/article/pii/S0143816607002266.

[127] Z. Wei, M. Shao, G. Zhang, Y. Wang, Parallel-based calibration method for line-structured light vision sensor, Opt. Eng. 53 (3) (2014) 1–13, http://dx.doi.org/10.1117/1.OE.53.3.033101.

[128] M. Rufli, D. Scaramuzza, R. Siegwart, Automatic detection of checkerboards on blurred and distorted images, in: 2008 IEEE/RSJ International Conference on Intelligent Robots and Systems, 2008, pp. 3121–3126, http://dx.doi.org/10.1109/IROS.2008.4650703.

[129] S. Lee, S. Lee, J. Choi, Correction of radial distortion using a planar checkerboard pattern and its image, IEEE Trans. Consum. Electron. 55 (1) (2009) 27–33, http://dx.doi.org/10.1109/TCE.2009.4814410.

[130] Q. Chen, H. Wu, T. Wada, Camera calibration with two arbitrary coplanar circles, in: Lecture Notes in Computer Science Computer Vision - ECCV 2004, 2004, pp. 521–532, http://dx.doi.org/10.1007/978-3-540-24672-5_41.

[131] G. Jiang, L. Quan, Detection of concentric circles for camera calibration, in: Tenth IEEE International Conference on Computer Vision, Vol. 1, ICCV'05, IEEE, 2005, pp. 333–340.

[132] C. Colombo, D. Comanducci, A. Del Bimbo, Camera calibration with two arbitrary coaxial circles, in: European Conference on Computer Vision, Springer, 2006, pp. 265–276.

[133] Y. Wu, H. Zhu, Z. Hu, F. Wu, Camera calibration from the quasi-affine invariance of two parallel circles, in: European Conference on Computer Vision, Springer, 2004, pp. 190–202.

[134] J. Guan, F. Deboeverie, M. Slembrouck, D. Haerenborgh, D. Cauwelaert, P. Veelaert, W. Philips, Extrinsic calibration of camera networks using a sphere, Sensors (Basel, Switzerland) 15 (2015) 18985–19005, http://dx.doi.org/10.3390/s150818985.

[135] L. Huang, F. Da, S. Gai, Research on multi-camera calibration and point cloud correction method based on three-dimensional calibration object, Opt. Lasers Eng. 115 (2019) 32–41, http://dx.doi.org/10.1016/j.optlaseng.2018.11.005, URL: https://www.sciencedirect.com/science/article/pii/S0143816618308273.

[136] T. Xue, B. Wu, J. Zhu, S. Ye, Complete calibration of a structure-uniform stereovision sensor with free-position planar pattern, Sensors Actuators A 135 (1) (2007) 185–191, http://dx.doi.org/10.1016/j.sna.2006.07.004, URL: https://www.sciencedirect.com/science/article/pii/S0924424706004869, Special Issue of The Micromechanics section of Sensors and Actuators (SAMM, based on contributions revised from the Technical Digest of the IEEE 19th International conference on Micro Electro Mechanical Systems (MEMS 2006)).

[137] G. Koo, W. Jung, N. Doh, A two-step optimization for extrinsic calibration of multiple camera system (MCS) using depth-weighted normalized points, IEEE Robot. Autom. Lett. 6 (4) (2021) 6608–6615.

[138] K.K. Wong, G. Zhang, Z. Chen, A stratified approach for camera calibration using spheres, IEEE Trans. Image Process. 20 (2) (2011) 305–316, http://dx.doi.org/10.1109/TIP.2010.2063035.

[139] Z. Liu, G. Zhang, Z. Wei, J. Sun, Novel calibration method for non-overlapping multiple vision sensors based on 1D target, Opt. Lasers Eng. 49 (4) (2011) 570–577, http://dx.doi.org/10.1016/j.optlaseng.2010.11.002, URL: https://www.sciencedirect.com/science/article/pii/S0143816610002460.

[140] J. Sun, Q. Liu, Z. Liu, G. Zhang, A calibration method for stereo vision sensor with large FOV based on 1D targets, Opt. Lasers Eng. 49 (11) (2011) 1245–1250, http://dx.doi.org/10.1016/j.optlaseng.2011.06.011, URL: https://www.sciencedirect.com/science/article/pii/S0143816611001898.

[141] M. Xie, Z. Wei, G. Zhang, X. Wei, A flexible technique for calibrating relative position and orientation of two cameras with no-overlapping FOV, Measurement 46 (1) (2013) 34–44, http://dx.doi.org/10.1016/j.measurement.2012.10.005, URL: https://www.sciencedirect.com/science/article/pii/S0263224112003776.

[142] Z. Liu, G. Zhang, Z. Wei, J. Sun, A global calibration method for multiple vision sensors based on multiple targets, Meas. Sci. Technol. 22 (12) (2011) 125102, http://dx.doi.org/10.1088/0957-0233/22/12/125102.

[143] T. Strauß, J. Ziegler, J. Beck, Calibrating multiple cameras with non-overlapping views using coded checkerboard targets, in: 17th International IEEE Conference on Intelligent Transportation Systems, ITSC, 2014, pp. 2623–2628, http://dx.doi.org/10.1109/ITSC.2014.6958110.

[144] J. Zhang, J. Zhu, H. Deng, Z. Chai, M. Ma, X. Zhong, Multi-camera calibration method based on a multi-plane stereo target, Appl. Opt. 58 (34) (2019) 9353–9359, http://dx.doi.org/10.1364/AO.58.009353, URL: http://ao.osa.org/abstract.cfm?URI=ao-58-34-9353.

[145] R.K. Kumar, A. Ilie, J.-M. Frahm, M. Pollefeys, Simple calibration of non-overlapping cameras with a mirror, in: 2008 IEEE Conference on Computer Vision and Pattern Recognition, IEEE, 2008, pp. 1–7.

[146] K. Takahashi, S. Nobuhara, T. Matsuyama, A new mirror-based extrinsic camera calibration using an orthogonality constraint, in: 2012 IEEE Conference on Computer Vision and Pattern Recognition, 2012, pp. 1051–1058, http://dx.doi.org/10.1109/CVPR.2012.6247783.

[147] A. Agrawal, Extrinsic camera calibration without a direct view using spherical mirror, in: 2013 IEEE International Conference on Computer Vision, 2013, pp. 2368–2375, http://dx.doi.org/10.1109/ICCV.2013.294.

[148] S. Fujiyama, F. Sakaue, J. Sato, Multiple view geometries for mirrors and cameras, in: 2010 20th International Conference on Pattern Recognition, 2010, pp. 45–48, http://dx.doi.org/10.1109/ICPR.2010.20.

[149] G.L. Mariottini, S. Scheggi, F. Morbidi, D. Prattichizzo, Planar mirrors for image-based robot localization and 3-D reconstruction, Mechatronics 22 (4) (2012) 398–409, http://dx.doi.org/10.1016/j.mechatronics.2011.09.004, URL: https://www.sciencedirect.com/science/article/pii/S0957415811001474, Visual Servoing SI.

[150] J. Gluckman, S.K. Nayar, Catadioptric stereo using planar mirrors, Int. J. Comput. Vis. 44 (1) (2001) 65–79, http://dx.doi.org/10.1023/a:1011172403203, URL: https://link.springer.com/article/10.1023/A:1011172403203#citeas.

[151] Z. Xu, Y. Wang, C. Yang, Multi-camera global calibration for large-scale measurement based on plane mirror, Optik 126 (23) (2015) 4149–4154, http://dx.doi.org/10.1016/j.ijleo.2015.08.015, URL: https://www.sciencedirect.com/science/article/pii/S0030402615007743.

[152] S. Wasielewski, O. Strauss, Calibration of a multi-sensor system laser rangefinder/camera, in: Proceedings of the Intelligent Vehicles' 95. Symposium, IEEE, 1995, pp. 472–477.

[153] G. Li, Y. Liu, L. Dong, X. Cai, D. Zhou, An algorithm for extrinsic parameters calibration of a camera and a laser range finder using line features, in: 2007 IEEE/RSJ International Conference on Intelligent Robots and Systems, IEEE, 2007, pp. 3854–3859.

[154] K. Kwak, D.F. Huber, H. Badino, T. Kanade, Extrinsic calibration of a single line scanning LiDAR and a camera, in: 2011 IEEE/RSJ International Conference on Intelligent Robots and Systems, IEEE, 2011, pp. 3283–3289.

[155] Qilong Zhang, R. Pless, Extrinsic calibration of a camera and laser range finder (improves camera calibration), in: 2004 IEEE/RSJ International Conference on Intelligent Robots and Systems (IROS) (IEEE Cat. No.04CH37566), Vol. 3, IEEE, 2004, pp. 2301–2306, http://dx.doi.org/10.1109/IROS.2004.1389752, URL: http://ieeexplore.ieee.org/document/1389752/.

[156] O. Naroditsky, A. Patterson, K. Daniilidis, Automatic alignment of a camera with a line scan LiDAR system, in: 2011 IEEE International Conference on Robotics and Automation, IEEE, 2011, pp. 3429–3434.

[157] F. Vasconcelos, J.P. Barreto, U. Nunes, A minimal solution for the extrinsic calibration of a camera and a laser-rangefinder, IEEE Trans. Pattern Anal. Mach. Intell. 34 (11) (2012) 2097–2107.

[158] R. Gomez-Ojeda, J. Briales, E. Fernandez-Moral, J. Gonzalez-Jimenez, Extrinsic calibration of a 2D laser-rangefinder and a camera based on scene corners, in: 2015 IEEE International Conference on Robotics and Automation, ICRA, IEEE, 2015, pp. 3611–3616.

[159] Z. Hu, Y. Li, N. Li, B. Zhao, Extrinsic calibration of 2-D laser rangefinder and camera from single shot based on minimal solution, IEEE Trans. Instrum. Meas. 65 (4) (2016) 915–929.

[160] W. Dong, V. Isler, A novel method for the extrinsic calibration of a 2D laser rangefinder and a camera, IEEE Sens. J. 18 (10) (2018) 4200–4211.

[161] S. Kato, S. Tokunaga, Y. Maruyama, S. Maeda, M. Hirabayashi, Y. Kitsukawa, A. Monrroy, T. Ando, Y. Fujii, T. Azumi, Autoware on board: Enabling autonomous vehicles with embedded systems, in: Proceedings of the 9th ACM/IEEE International Conference on Cyber-Physical Systems, ICCPS '18, IEEE Press, 2018, pp. 287–296, http://dx.doi.org/10.1109/ICCPS.2018.00035.

[162] Baidu, ApolloAuto, 2020, GitHub, URL: https://github.com/ApolloAuto/apollo, (Accessed: 31 August 2022).

[163] A. Dhall, K. Chelani, V. Radhakrishnan, K.M. Krishna, Lidar-camera calibration using 3D-3D point correspondences, 2017, CoRR abs/1705.09785, URL: http://arxiv.org/abs/1705.09785.

[164] L. Zhou, Z. Deng, Extrinsic calibration of a camera and a LiDAR based on decoupling the rotation from the translation, in: 2012 IEEE Intelligent Vehicles Symposium, IEEE, 2012, pp. 642–648.

[165] J.-E. Ha, Extrinsic calibration of a camera and laser range finder using a new calibration structure of a plane with a triangular hole, Int. J. Control Autom. Syst. 10 (6) (2012) 1240–1244.

[166] M. Velas, M. Spanel, Z. Materna, A. Herout, Calibration of RGB camera with velodyne LiDAR, in: WSCG 2014 Communication Papers Proceedings, Václav Skala-UNION Agency, 2014, pp. 135–144.

[167] J. Kümmerle, T. Kühner, M. Lauer, Automatic calibration of multiple cameras and depth sensors with a spherical target, in: 2018 IEEE/RSJ International Conference on Intelligent Robots and Systems, IROS, IEEE, 2018, pp. 1–8.

[168] G. Pandey, J. McBride, S. Savarese, R. Eustice, Extrinsic calibration of a 3D laser scanner and an omnidirectional camera, IFAC Proc. Vol. 43 (16) (2010) 336–341.

[169] W. Wang, K. Sakurada, N. Kawaguchi, Reflectance intensity assisted automatic and accurate extrinsic calibration of 3D LiDAR and panoramic camera using a printed chessboard, Remote Sens. 9 (8) (2017) 851.

[170] L. Zhou, Z. Li, M. Kaess, Automatic extrinsic calibration of a camera and a 3D LiDAR using line and plane correspondences, in: 2018 IEEE/RSJ International Conference on Intelligent Robots and Systems, IROS, IEEE, 2018, pp. 5562–5569.

[171] Z. Lai, Y. Wang, S. Guo, X. Meng, J. Li, W. Li, S. Han, Laser reflectance feature assisted accurate extrinsic calibration for non-repetitive scanning LiDAR and camera systems, Opt. Express 30 (10) (2022) 16242–16263, http://dx.doi.org/10.1364/OE.453449, URL: http://opg.optica.org/oe/abstract.cfm?URI=oe-30-10-16242.

[172] Y. Park, S. Yun, C.S. Won, K. Cho, K. Um, S. Sim, Calibration between color camera and 3D LIDAR instruments with a polygonal planar board, Sensors 14 (3) (2014) 5333–5353.

[173] L. Grammatikopoulos, A. Papanagnou, A. Venianakis, I. Kalisperakis, C. Stentoumis, An effective camera-to-LiDAR spatiotemporal calibration based on a simple calibration target, Sensors 22 (15) (2022) http://dx.doi.org/10.3390/s22155576, URL: https://www.mdpi.com/1424-8220/22/15/5576.

[174] S. Yoon, S. Ju, H.M. Nguyen, S. Park, J. Heo, Spatiotemporal calibration of camera-LiDAR using nonlinear angular constraints on multiplanar target, IEEE Sens. J. 22 (11) (2022) 10995–11005, http://dx.doi.org/10.1109/JSEN.2022.3168860.

[175] X. Gong, Y. Lin, J. Liu, 3D LIDAR-camera extrinsic calibration using an arbitrary trihedron, Sensors (Switzerland) 13 (2) (2013) 1902–1918, http://dx.doi.org/10.3390/s130201902.

[176] V. Fremont, P. Bonnifait, Extrinsic calibration between a multi-layer LiDAR and a camera, in: 2008 IEEE International Conference on Multisensor Fusion and Integration for Intelligent Systems, IEEE, 2008, pp. 214–219.

[177] Z. Pusztai, L. Hajder, Accurate calibration of LiDAR-camera systems using ordinary boxes, in: Proceedings of the IEEE International Conference on Computer Vision Workshops, 2017, pp. 394–402.

[178] Z. Pusztai, I. Eichhardt, L. Hajder, Accurate calibration of multi-LiDAR-multi-camera systems, Sensors (Basel, Switzerland) 18 (2018).

[179] A. Povendhan, L. Yi, A. Hayat, A.V. Le, K. Kai, B. Ramalingam, M. Elara, Multi-sensor fusion incorporating adaptive transformation for reconfigurable pavement sweeping robot, in: 2021 IEEE/RSJ International Conference on Intelligent Robots and Systems, IROS, IEEE, 2021, pp. 300–306.

[180] G. Zamanakos, L. Tsochatzidis, A. Amanatiadis, I. Pratikakis, A cooperative LiDAR-camera scheme for extrinsic calibration, in: 2022 IEEE 14th Image, Video, and Multidimensional Signal Processing Workshop, IVMSP, IEEE, 2022, pp. 1–5.

[181] C. Fang, S. Ding, Z. Dong, H. Li, S. Zhu, P. Tan, Single-shot is enough: Panoramic infrastructure based calibration of multiple cameras and 3D LiDARs, in: 2021 IEEE/RSJ International Conference on Intelligent Robots and Systems, IROS, 2021, pp. 8890–8897, http://dx.doi.org/10.1109/IROS51168.2021.9636767.

[182] H. Zhao, Y. Chen, R. Shibasaki, An efficient extrinsic calibration of a multiple laser scanners and cameras' sensor system on a mobile platform, in: 2007 IEEE Intelligent Vehicles Symposium, IEEE, 2007, pp. 422–427.

[183] D. Scaramuzza, A. Harati, R. Siegwart, Extrinsic self calibration of a camera and a 3D laser range finder from natural scenes, in: 2007 IEEE/RSJ International Conference on Intelligent Robots and Systems, IEEE, 2007, pp. 4164–4169.

[184] D.L. Hill, P.G. Batchelor, M. Holden, D.J. Hawkes, Medical image registration, Phys. Med. Biol. 46 (3) (2001) R1.

[185] A. Mastin, J. Kepner, J. Fisher, Automatic registration of LIDAR and optical images of urban scenes, in: 2009 IEEE Conference on Computer Vision and Pattern Recognition, IEEE, 2009, pp. 2639–2646.

[186] E.G. Parmehr, C.S. Fraser, C. Zhang, J. Leach, Automatic registration of optical imagery with 3D LiDAR data using statistical similarity, ISPRS J. Photogramm. Remote Sens. 88 (2014) 28–40.

[187] G. Pandey, J.R. Mcbride, S. Savarese, R.M. Eustice, Automatic extrinsic calibration of vision and LiDAR by maximizing mutual information, J. Field Robotics 32 (5) (2014) 696–722, http://dx.doi.org/10.1002/rob.21542.

[188] C. Yuan, X. Liu, X. Hong, F. Zhang, Pixel-level extrinsic self calibration of high resolution LiDAR and camera in targetless environments, IEEE Robot. Autom. Lett. 6 (4) (2021) 7517–7524.

[189] X. Liu, C. Yuan, F. Zhang, Targetless extrinsic calibration of multiple small FoV LiDARs and cameras using adaptive voxelization, IEEE Trans. Instrum. Meas. 71 (2022) 1–12, http://dx.doi.org/10.1109/TIM.2022.3176889.

[190] Z. Taylor, J. Nieto, A mutual information approach to automatic calibration of camera and LiDAR in natural environments, in: Australian Conference on Robotics and Automation, 2012, pp. 3–5.

[191] Z. Taylor, J. Nieto, D. Johnson, Multi-modal sensor calibration using a gradient orientation measure, J. Field Robotics 32 (5) (2015) 675–695.

[192] K. Irie, M. Sugiyama, M. Tomono, Target-less camera-LiDAR extrinsic calibration using a bagged dependence estimator, in: 2016 IEEE International Conference on Automation Science and Engineering, CASE, IEEE, 2016, pp. 1340–1347.

[193] K. Koide, S. Oishi, M. Yokozuka, A. Banno, General, single-shot, target-less, and automatic LiDAR-camera extrinsic calibration toolbox, 2023, arXiv preprint arXiv:2302.05094.

[194] X.-S. Gao, X.-R. Hou, J. Tang, H.-F. Cheng, Complete solution classification for the perspective-three-point problem, IEEE Trans. Pattern Anal. Mach. Intell. 25 (8) (2003) 930–943.

[195] X. Zhao, W. Chen, Z. Liu, X. Ma, L. Kong, X. Wu, H. Yue, X. Yan, LiDAR-ToF-Binocular depth fusion using gradient priors, in: 2020 Chinese Control and Decision Conference, CCDC, IEEE, 2020, pp. 2024–2029.

[196] J. Domhof, J.F. Kooij, D.M. Gavrila, An extrinsic calibration tool for radar, camera and LiDAR, in: 2019 International Conference on Robotics and Automation, ICRA, IEEE, 2019, pp. 8107–8113.

[197] J. Peršić, I. Marković, I. Petrović, Extrinsic 6dof calibration of a radar–LiDAR–camera system enhanced by radar cross section estimates evaluation, Robot. Auton. Syst. 114 (2019) 217–230.

[198] J. Zhang, P. Siritanawan, Y. Yue, C. Yang, M. Wen, D. Wang, A two-step method for extrinsic calibration between a sparse 3D LiDAR and a thermal camera, in: 2018 15th International Conference on Control, Automation, Robotics and Vision, ICARCV, IEEE, 2018, pp. 1039–1044.

[199] Y. Cai, Y. Zhou, H. Zhang, Y. Xia, P. Qiao, J. Zhao, Review of target geo-location algorithms for aerial remote sensing cameras without control points, Appl. Sci. 12 (24) (2022) 12689.

[200] G. Bai, Y. Song, Y. Zuo, M. Song, X. Wang, Multitarget location capable of adapting to complex geomorphic environment for the airborne photoelectric reconnaissance system, J. Appl. Remote Sens. 14 (3) (2020) 036510.

[201] D. Song, R. Tharmarasa, W. Wang, B. Rao, D. Brown, T. Kirubarajan, Efficient bias estimation in airborne video georegistration for ground target tracking, IEEE Trans. Aerosp. Electron. Syst. 57 (5) (2021) 3198–3208.

[202] M. Oliveira, E. Pedrosa, A.P. de Aguiar, D.F.P.D. Rato, F.N. dos Santos, P. Dias, V. Santos, ATOM: A general calibration framework for multi-modal, multi-sensor systems, Expert Syst. Appl. 207 (2022) 118000, http://dx.doi.org/10.1016/j.eswa.2022.118000, URL: https://www.sciencedirect.com/science/article/pii/S0957417422012234.

[203] D. Rato, M. Oliveira, V. Santos, M. Gomes, A. Sappa, A sensor-to-pattern calibration framework for multi-modal industrial collaborative cells, J. Manuf. Syst. 64 (2022) 497–507, http://dx.doi.org/10.1016/j.jmsy.2022.07.006, URL: https://www.sciencedirect.com/science/article/pii/S0278612522001182.

[204] J. Elseberg, D. Borrmann, A. Nüchter, Algorithmic solutions for computing precise maximum likelihood 3D point clouds from mobile laser scanning platforms, Remote Sens. 5 (11) (2013) 5871–5906.

[205] D.A. Cucci, M. Matteucci, Position tracking and sensors self-calibration in autonomous mobile robots by Gauss-Newton optimization, in: 2014 IEEE International Conference on Robotics and Automation, ICRA, IEEE, 2014, pp. 1269–1275.

[206] D.A. Cucci, M. Rehak, J. Skaloud, Bundle adjustment with raw inertial observations in UAV applications, ISPRS J. Photogramm. Remote Sens. 130 (2017) 1–12.
[207] S. Lynen, M.W. Achtelik, S. Weiss, M. Chli, R. Siegwart, A robust and modular multi-sensor fusion approach applied to MAV navigation, in: 2013 IEEE/RSJ International Conference on Intelligent Robots and Systems, IEEE, 2013, pp. 3923–3929.
[208] S. Shen, Y. Mulgaonkar, N. Michael, V. Kumar, Multi-sensor fusion for robust autonomous flight in indoor and outdoor environments with a rotorcraft MAV, in: 2014 IEEE International Conference on Robotics and Automation, ICRA, IEEE, 2014, pp. 4974–4981.
[209] W. Lee, Y. Yang, G. Huang, Efficient multi-sensor aided inertial navigation with online calibration, in: 2021 IEEE International Conference on Robotics and Automation, ICRA, IEEE, 2021, pp. 5706–5712.
[210] T. Zhou, S.M. Hasheminasab, A. Habib, Tightly-coupled camera/LiDAR integration for point cloud generation from GNSS/INS-assisted UAV mapping systems, ISPRS J. Photogramm. Remote Sens. 180 (2021) 336–356.
[211] W. Lee, Y. Yang, G. Huang, Efficient multi-sensor aided inertial navigation with online calibration, in: 2021 IEEE International Conference on Robotics and Automation, ICRA, IEEE, 2021, pp. 5706–5712.
[212] J. Rehder, R. Siegwart, P. Furgale, A general approach to spatiotemporal calibration in multisensor systems, IEEE Trans. Robot. 32 (2) (2016) 383–398.
[213] E. Mair, M. Fleps, M. Suppa, D. Burschka, Spatio-temporal initialization for IMU to camera registration, in: 2011 IEEE International Conference on Robotics and Biomimetics, IEEE, 2011, pp. 557–564.
[214] J. Peršić, L. Petrović, I. Marković, I. Petrović, Spatiotemporal multisensor calibration via Gaussian processes moving target tracking, IEEE Trans. Robot. (2021).
[215] K. Qiu, T. Qin, J. Pan, S. Liu, S. Shen, Real-time temporal and rotational calibration of heterogeneous sensors using motion correlation analysis, IEEE Trans. Robot. 37 (2) (2020) 587–602.
[216] R. Ravi, Y.-J. Lin, M. Elbahnasawy, T. Shamseldin, A. Habib, Simultaneous system calibration of a multi-LiDAR multicamera mobile mapping platform, IEEE J. Sel. Top. Appl. Earth Obs. Remote Sens. 11 (5) (2018) 1694–1714.
[217] F. Lian, C. Han, W. Liu, H. Chen, Joint spatial registration and multi-target tracking using an extended probability hypothesis density filter, IET Radar Sonar Navig. 5 (4) (2011) 441–448.
[218] L. Gao, J. Huang, W. Sun, P. Wei, H. Liao, Multi-sensor multi-target Bernoulli filter with registration biases, IEICE Trans. Fundam. Electron. Commun. Comput. Sci. 99 (10) (2016) 1774–1781.
[219] M. Li, Z. Jing, H. Pan, P. Dong, Joint registration and multi-target tracking based on labelled random finite set and expectation maximisation, IET Radar Sonar Navig. 12 (3) (2018) 312–322.
[220] M. Üney, B. Mulgrew, D.E. Clark, A cooperative approach to sensor localisation in distributed fusion networks, IEEE Trans. Signal Process. 64 (5) (2015) 1187–1199.
[221] L. Gao, G. Battistelli, L. Chisci, A.K. Gostar, R. Hoseinnezhad, Distributed joint mapping and registration with limited fields-of-view, in: 2019 International Conference on Control, Automation and Information Sciences, ICCAIS, IEEE, 2019, pp. 1–6.
[222] L. Gao, G. Battistelli, L. Chisci, P. Wei, Distributed joint sensor registration and target tracking via sensor network, Inf. Fusion 46 (2019) 218–230.
[223] C. Guindel, J. Beltrán, D. Martín, F. García, Automatic extrinsic calibration for LiDAR-stereo vehicle sensor setups, in: 2017 IEEE 20th International Conference on Intelligent Transportation Systems, ITSC, IEEE, 2017, pp. 1–6.
[224] A. Geiger, F. Moosmann, Ö. Car, B. Schuster, Automatic camera and range sensor calibration using a single shot, in: 2012 IEEE International Conference on Robotics and Automation, IEEE, 2012, pp. 3936–3943.
[225] B. Nagy, L. Kovács, C. Benedek, Online targetless end-to-end camera-LiDAR self-calibration, in: 2019 16th International Conference on Machine Vision Applications, MVA, IEEE, 2019, pp. 1–6.
[226] J.L. Owens, P.R. Osteen, K. Daniilidis, MSG-Cal: Multi-sensor graph-based calibration, in: 2015 IEEE/RSJ International Conference on Intelligent Robots and Systems, IROS, IEEE, 2015, pp. 3660–3667.
[227] A. Bonci, P.D. Cen Cheng, M. Indri, G. Nabissi, F. Sibona, Human-robot perception in industrial environments: A survey, Sensors 21 (5) (2021) 1571.
[228] Y. Xu, Z. Wang, Visual sensing technologies in robotic welding: Recent research developments and future interests, Sensors Actuators A 320 (2021) 112551.
[229] H. Ahmed, H.M. La, N. Gucunski, Review of non-destructive civil infrastructure evaluation for bridges: State-of-the-art robotic platforms, sensors and algorithms, Sensors 20 (14) (2020) 3954.
[230] Y. Tian, C. Chen, K. Sagoe-Crentsil, J. Zhang, W. Duan, Intelligent robotic systems for structural health monitoring: Applications and future trends, Autom. Constr. 139 (2022) 104273.
[231] S. Fountas, N. Mylonas, I. Malounas, E. Rodias, C. Hellmann Santos, E. Pekkeriet, Agricultural robotics for field operations, Sensors 20 (9) (2020) 2672.
[232] G. Ren, T. Lin, Y. Ying, G. Chowdhary, K. Ting, Agricultural robotics research applicable to poultry production: A review, Comput. Electron. Agric. 169 (2020) 105216.
[233] Q. Chen, Y. Xie, S. Guo, J. Bai, Q. Shu, Sensing system of environmental perception technologies for driverless vehicle: A review of state of the art and challenges, Sensors Actuators A 319 (2021) 112566.
[234] P. Kolar, P. Benavidez, M. Jamshidi, Survey of datafusion techniques for laser and vision based sensor integration for autonomous navigation, Sensors 20 (8) (2020) 2180.
[235] L. Liu, X. Guo, C. Lee, Promoting smart cities into the 5G era with multi-field Internet of Things (IoT) applications powered with advanced mechanical energy harvesters, Nano Energy 88 (2021) 106304.
[236] S. Samaras, E. Diamantidou, D. Ataloglou, N. Sakellariou, A. Vafeiadis, V. Magoulianitis, A. Lalas, A. Dimou, D. Zarpalas, K. Votis, et al., Deep learning on multi sensor data for counter UAV applications—A systematic review, Sensors 19 (22) (2019) 4837.
[237] M.A. Azam, K.B. Khan, S. Salahuddin, E. Rehman, S.A. Khan, M.A. Khan, S. Kadry, A.H. Gandomi, A review on multimodal medical image fusion: Compendious analysis of medical modalities, multimodal databases, fusion techniques and quality metrics, Comput. Biol. Med. 144 (2022) 105253.
[238] R. Gravina, P. Alinia, H. Ghasemzadeh, G. Fortino, Multi-sensor fusion in body sensor networks: State-of-the-art and research challenges, Inf. Fusion 35 (2017) 68–80.
[239] S. Luo, Q. Meng, S. Li, H. Yu, Research of intent recognition in rehabilitation robots: A systematic review, Disabil. Rehabil.: Assist. Technol. (2023) 1–12.
[240] S. Mishra, P.R. Osteen, G. Pandey, S. Saripalli, Experimental evaluation of 3D-LiDAR camera extrinsic calibration, in: 2020 IEEE/RSJ International Conference on Intelligent Robots and Systems, IROS, IEEE, 2020, pp. 9020–9026.
[241] J. Kang, N.L. Doh, Automatic targetless camera–LIDAR calibration by aligning edge with Gaussian mixture model, J. Field Robotics 37 (1) (2020) 158–179.
[242] S. Nedevschi, et al., Online cross-calibration of camera and LiDAR, in: 2017 13th IEEE International Conference on Intelligent Computer Communication and Processing, ICCP, IEEE, 2017, pp. 295–301.
[243] Z. Bu, C. Sun, P. Wang, H. Dong, Calibration of camera and flash LiDAR system with a triangular pyramid target, Appl. Sci. 11 (2) (2021) 582.
[244] A. Li, D. Zou, W. Yu, Robust initialization of multi-camera slam with limited view overlaps and inaccurate extrinsic calibration, in: 2021 IEEE/RSJ International Conference on Intelligent Robots and Systems, IROS, IEEE, 2021, pp. 3361–3367.
[245] D. Wang, Q. Pan, C. Zhao, J. Hu, L. Liu, L. Tian, SLAM-based cooperative calibration for optical sensors array with GPS/IMU aided, in: 2016 International Conference on Unmanned Aircraft Systems, ICUAS, IEEE, 2016, pp. 615–623.
[246] M.Á. Muñoz-Bañón, F.A. Candelas, F. Torres, Targetless camera-LiDAR calibration in unstructured environments, IEEE Access 8 (2020) 143692–143705.
[247] K. Ebadi, Y. Chang, M. Palieri, A. Stephens, A. Hatteland, E. Heiden, A. Thakur, N. Funabiki, B. Morrell, S. Wood, et al., LAMP: Large-scale autonomous mapping and positioning for exploration of perceptually-degraded subterranean environments, in: 2020 IEEE International Conference on Robotics and Automation, ICRA, IEEE, 2020, pp. 80–86.
[248] Z. Xiao, H. Li, D. Zhou, Y. Dai, B. Dai, Accurate extrinsic calibration between monocular camera and sparse 3D LiDAR points without markers, in: 2017 IEEE Intelligent Vehicles Symposium, IV, IEEE, 2017, pp. 424–429.
[249] J. Zhang, R. Zhang, Y. Yue, C. Yang, M. Wen, D. Wang, Slat-calib: Extrinsic calibration between a sparse 3D LiDAR and a limited-fov low-resolution thermal camera, in: 2019 IEEE International Conference on Robotics and Biomimetics, ROBIO, IEEE, 2019, pp. 648–653.
[250] P. An, T. Ma, K. Yu, B. Fang, J. Zhang, W. Fu, J. Ma, Geometric calibration for LiDAR-camera system fusing 3D-2D and 3D-3D point correspondences, Opt. Express 28 (2) (2020) 2122–2141.
[251] D. Bender, M. Schikora, J. Sturm, D. Greniers, Ins-camera calibration without ground control points, in: 2014 Sensor Data Fusion: Trends, Solutions, Applications, SDF, IEEE, 2014, pp. 1–6.
[252] E. Wise, J. Peršić, C. Grebe, I. Petrović, J. Kelly, A continuous-time approach for 3D radar-to-camera extrinsic calibration, in: 2021 IEEE International Conference on Robotics and Automation, ICRA, IEEE, 2021, pp. 13164–13170.
[253] M. Li, A.I. Mourikis, Online temporal calibration for camera–IMU systems: Theory and algorithms, Int. J. Robot. Res. 33 (7) (2014) 947–964.
[254] T. Qin, S. Shen, Online temporal calibration for monocular visual-inertial systems, in: 2018 IEEE/RSJ International Conference on Intelligent Robots and Systems, IROS, IEEE, 2018, pp. 3662–3669.